

FINAL PROJECT REPORT

Assessment of the Tri-potential
Electrical Resistivity Survey in Defining
Cavities, Fracture Zones and Aquifers

by

Keith Kirk and Dr. Henry Rauch

1976

TABLE OF CONTENTS

	Page
List of Figures	1
Introduction.	2
Literature Review	4
Basic Theoretical Considerations.	8
General Concepts	8
Electrode Configurations	13
The Tri-Potential Arrays	16
Field Techniques and Theory	19
Depth Sounding Tri-Potential Survey.	19
Profiling Tri-Potential Survey	20
Fracture Zones	21
Cavities	28
Field Results	34
Profiling Tri-Potential Survey	34
Depth Sounding Survey.	39
Resistivity Modeling	43
Conclusions	45
General Conclusions.	45
Conclusions for U.G.C. Site.	46
Selected References	48
Appendix A.	51
Appendix B.	59

LIST OF FIGURES

Figure	Page
1 A General Electrode Configuration	10
2 Various Electrode Arrays.	12
3 Logn Electrode Configuration.	15
4 $C_1C_2P_1P_2$ and $C_1P_1C_2P_2$ Electrode Configurations.	18
5 Theoretical Tri-potential Profile Across a Vertical Infinite Insulating Plane.	24
6 Effect of Positive Resistivity Contrasts on Anomaly Associated With Fracture Trace	25
7 Effect of Negative Resistivity Contrasts on Anomaly Associated With Traverse Across Fracture Zone.	26
8 The Effect of Variations of Fracture Width on the Resistivity Profile for a Constant Resistivity Contrast of +0.6 for cppc Array.	27
9 Effect of Electrode Separation on the Resistivity Profile Across a Vertical Fracture Zone.	29
10 Tri-potential Resistivity Response to Perfectly Insulating Sphere.	31
11 Chart Relating $\rho_{\text{cppc}_{\text{MAX}}}/\rho_{\infty}$ and $\rho_{\text{cpcp}_a}/\rho_{\infty}$ Response to Electrode Spacing (a) Sphere Radius (r) and Top of Sphere (H).	33
12 Outline of Drainage Basins Containing the Underground Coal Gasification (U.G.U.) site, modified after Sole et al. (1976)	35
13 Map of Fracture Zones Located by Tri-potential Earth Resistivity Survey USBM-UGC Site, Wetzel County, West Virginia.	*
14 Segment of Tri-potential Resistivity Profile H-H' Showing Effect of Two Shallow Fractures.	*
15 Segment of Tri-potential Resistivity Profile D-D' Showing Effect of a Deep Fracture.	*
16 Plot of Apparent Resistivity and Tri-potential Residual versus Electrode Spacing for ERDA, MERC UGC site Depth Sounding Survey.	*
17 Plot of Apparent Resistivity versus Electrode Spacing for Modeled and Field Data	*

* Figure is in envelope at rear of report.

INTRODUCTION

The purpose of this report is to first review the theory, operation, and potential applications of the tri-potential method of resistivity survey, and then to report on how this geophysical survey method was used at the Morgantown Energy Research Center's underground coal gasification (U.G.C.) site in Wetzell County, West Virginia; the results and conclusions from this phase of the project are also presented. This research project was performed under grant number G0155012 as funded by the U.S. Energy Research and Development Administration.

The results of this study concerning the geophysical detection of fracture zones and caves in karst terrains and of ground-water aquifers in other terrains are not presented in this report. These results are instead available in Kirk (1976), on file at West Virginia University.

The idea for this research was gleaned by reading the papers of Habberjam (1969), Carpenter and Habberjam (1955), and Carpenter (1955), which basically outlined the methods of the tri-potential resistivity survey and suggested some possible applications and areas of further study. Of particular interest was the potential use of this technique in locating underground cavities and its applications to engineering geology and mining. Preliminary investigations by the author in the fall of 1973 indicated that this technique might also be readily applied to locating fracture zones and evaluating the water bearing nature of nonindurated sediments. It was at this time that the research was formulated and begun in earnest.

The research was designed in a standard type, three phase approach to the problem. These were:

Phase I Literature search and formulation of hypotheses.

Phase II Field investigations and testing of hypotheses.

Phase III Data reduction and conclusions.

Phase I was initiated in the fall of 1973 and continued in earnest until June of 1974. Phase II of this research started in the late fall of 1973, but the greatest bulk of field data was collected from June 1974 to March 1975. Phase III began in the fall of 1974 and continued until December 1975.

LITERATURE REVIEW

The tri-potential system for earth resistivity measurement was first discussed by Carpenter (1955); he proposed this method of survey to expediate the determination of lateral and local variations in earth resistivity. The tri-potential configuration was again discussed by Carpenter and Habberjam (1955), and for the first time this method of resistivity survey was given the name of tri-potential resistivity prospecting. In this paper the tri-potential method was described in detail, including the geometry of the system, the basic theory of the system, small scale brine tank modeling experiments, methods of computing theoretical curves given the Wenner curves, some small scale field experiments, and the development of the concept of tri-potential residual; these factors will be later discussed in greater detail. Habberjam (1969) used the tri-potential technique in a brine tank modeling experiment to determine the location, size, and depth of spherical cavities. His experiment proved successful and he was able to show a relationship between the response of two of the three electrode configurations involved in the tri-potential method and the depth and size of a spherical cavity. It was this research that encouraged the author of this thesis to initiate field investigations using the tri-potential method.

Resistivity measurements have been used extensively in the past to detect underground cavities. Most of this research has occurred

in karst areas when prospecting for caverns. In fact, resistivity surveys may be the most common geophysical tool used by karst researchers to date. Bates (1973), Dutta, et.al. (1970), Arandjelovic (1965), Bristow (1966), and Day (1964), have all used various methods of resistivity surveying to locate caverns in karst areas. Bates (1973) used a slight modification of the method employed by Bristow (1966) to locate caverns. In a homogeneous medium this method of cave detection has proved very successful in determining the map location and depth of the caverns.

Very little has been done using resistivity measurements to locate subterranean voids in other types of terrains, although Palmer (1954) used resistivity surveys to locate a railway tunnel in a sandstone-shale terrain, and H.R.B. - Singer Inc. in 1971 used resistivity surveys in an attempt to locate abandoned coal mines.

The resistivity survey has been used extensively to locate faults and fracture zones. Van Nostrand and Cook (1966) describe in detail the theoretical considerations behind locating faults and fracture traces using various electrode configurations including the Wenner, Lee, and Schlumberger configurations along with several asymmetrical configurations. They also include a thorough discussion of past work using resistivity profiling to locate faults and fracture traces. More recently, Merkel and Kaminski (1972) used a buried source resistivity technique to verify the presence of fracture zones first located by aerial photographs and in locating smaller fracture zones that had no surface expression. Stahl (1973, 1974) used the standard Wenner array to detect and delineate faults. This research is unique in that the resistivity surveys were followed

up by a detailed boring and core analysis that showed that the changes in resistivity correlated directly with changes in the rock structure in progressing over the fault zone.

Electrical resistivity surveying has been used extensively in unconsolidated material to delineate the bedrock interface below and to locate buried channels in glaciated areas for the purposes of water supply and engineering applications. At the present time, delineation of the bedrock-soil interface and buried channel locations are by far the most common application of electrical resistivity surveying. Buhle (1953) used resistivity to delineate zones where good ground-water supply would be most likely to occur. Here the fact was used that clean drinking water in sands and gravels has a relatively high resistivity value, while polluted water along with clay and silt have a lower resistance. Enslin (1953) used the standard Wenner array depth-sounding method to map the soil-bedrock interface in relation to foundation engineering design. Foster and Buhle (1951) in their classic paper used Wenner arrayed resistivity survey data in part for locating water wells with a great potential for high yields. Electric logs, geologic logs, and detailed geologic mapping were also used in this study. Since the late 1950's the development of computer technology has aided methods for interpretation of resistivity data, particularly for layered interpretations such as are used for soil-bedrock interface mapping and ground-water mapping. A very good recent text that gives detailed descriptions of the Schlumberger and Wenner surveys as well as calculations for layered interpretations is by Bhattachary and Patra (1968). A large

portion of this text deals with methods for calculating theoretical depth sounding profiles involving computer modeling. The electrical resistivity survey is becoming so common-place in the fields of ground-water prospecting and unconsolidated sediment mapping that little is found in the most recent literature on the more common techniques. Flathe (1963) outlined methods for generating five layer master curves specifically for hydrogeological interpretations where a salt water-fresh water interface exists. Flathe (1967, 1964) used these methods for detailed hydrogeological interpretation of resistivity data. More recently, Zohdy, Eaton and Mabey (1974) give a detailed methodology for the use of surface geophysics applied to ground-water investigations. Approximately one-third of this work was devoted to the use of resistivity as a method of ground-water investigation.

BASIC THEORETICAL CONSIDERATIONS

GENERAL CONCEPTS

In all methods of earth resistivity survey electric current is put into the ground artificially and the effects of this current on or within the ground are obtained by measurements of potential, differences in potential, or ratios of potential differences. One such potential value is then used with the known value of current input into the ground to calculate the resistance.

In a wire the resistance is directly proportional to its length and inversely proportional to its cross-sectional area. The constant of proportionality that relates the resistance to the length over the area of a wire is known as electrical resistivity. That is:

$$= R \cdot A / L \quad (1)$$

where: ρ = resistivity in ohm-feet or ohm-meters

R = resistance in ohms

A = area in ft² or meters²

L = length in feet or meters

The electrical resistivity is defined as the resistance of a given material of a given unit dimension.

In making resistivity surveys a square-waved alternating current (a.c.) of very low frequency (.1 to 6 hz) is impressed into the ground via two electrodes. Theoretically this low frequency a.c. current can be treated as direct current.

Using potential theory for a homogeneous, isotropic, semi-infinite half space, one can show that for a single current source the potential at any point in the half space is given by:

$$U = \rho \cdot I / 2 \cdot \pi \cdot R \quad (2)$$

where: U = potential

ρ = resistivity

R = distance from source to point of measurement

I = current

Because in the earth resistivity survey there is both a current source and current sink, the solution for the potential at a point must be calculated for this case. This is done by superposition since a current sink can be treated as a negative current source; hence for a two-electrode system the potential at a point in an isotropic homogeneous semi-infinite half space is given by:

$$U = I \cdot \rho / 2 \cdot \pi \cdot (1/R_1 - 1/R_2) \quad (3)$$

where: R_1 = distance from current source

R_2 = distance from current sink

Since in a resistivity survey a potential difference is measured using two more electrodes, the basic equation and superposition principle are applied again and this potential is defined as:

$$U = \rho \cdot I / 2 \cdot \pi \cdot (1/R_1 - 1/R_2 - 1/R_3 + 1/R_4) \quad (4)$$

where R_1 , R_2 , R_3 , and R_4 , are explained in Figure 1.

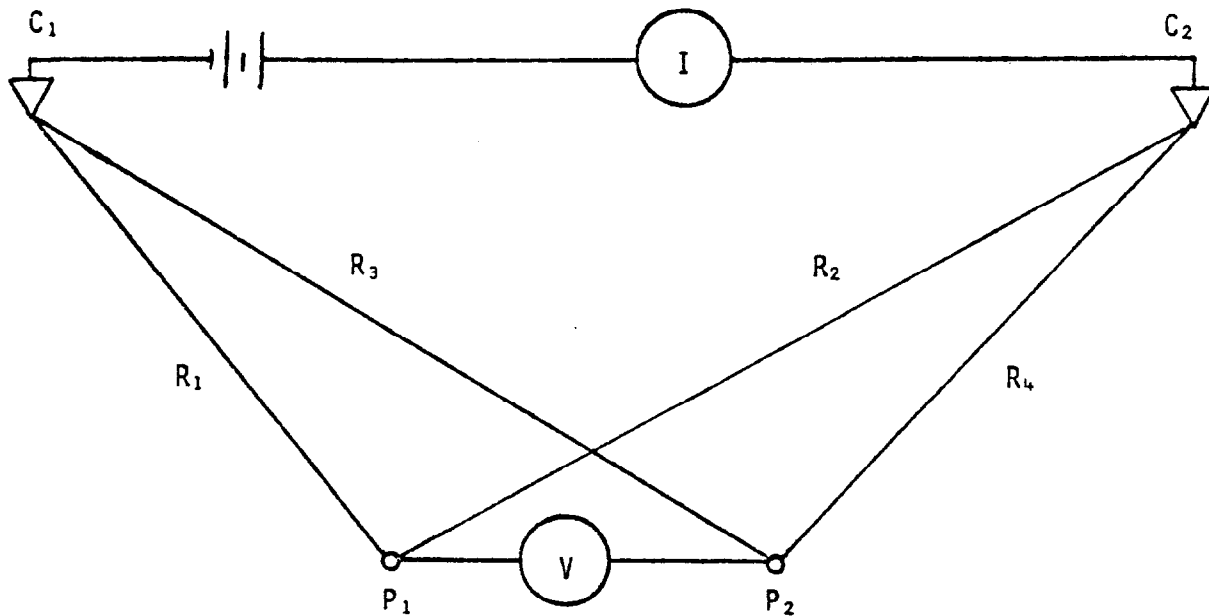


Figure 1: A general electrode configuration defining R_1 , R_2 , R_3 , R_4 as horizontal distances in plan view. C_1 and C_2 are current electrodes. P_1 and P_2 are potential electrodes.

Transposing Equation (4) for resistivity leads to:

$$\rho = 2 \cdot \pi \cdot U / I \cdot [1 / (1/R_1 - 1/R_2 - 1/R_3 + 1/R_4)] \quad (5)$$

The figure in brackets in Equation (5) depends only on the position of the electrodes and by definition is referred to as the configuration factor or geometry factor. From Equation (5), given the configuration factor only the potential difference and input current need to be known in order to determine the resistivity. That is to say, that for a given electrode setup, the configuration factor is a constant and the resistivity can be easily determined from Equation (5).

Given a particular electrode configuration and that configuration's geometry factor, the number of theoretical curves for a given hypothetical resistivity situation are greatly reduced. From Equation (5) it can be seen that the geometry factor is equal to:

$$G = 2 \cdot \pi / (1/R_1 - 1/R_2 - 1/R_3 + 1/R_4) \quad (6)$$

Using Equation (6) one may calculate the geometry factor for any four electrode resistivity array. The geometry factors for some of the more common arrays are listed below, where (a) and (b) are electrode spacings.

Wenner	$G = 2 \cdot \pi \cdot a$	(7)
--------	---------------------------	-----

Lee	$G = 4 \cdot \pi \cdot a$	(8)
-----	---------------------------	-----

Schlumberger	$G = \pi \cdot (a \cdot b + a^2) / b$	(9)
--------------	---------------------------------------	-----

Figure 2 illustrates the electrode configurations for the above-mentioned arrays plus the three configurations for the tri-potential array.

In any surface resistivity survey the quantity that is actually measured in the field is not the actual layer resistivity but a quantity known as the apparent resistivity. This measured apparent resistivity is a value that, for a given electrode configuration, represents the combined electrical effects produced by the various earth materials in close proximity to the electrodes. The apparent resistivity is a function of the electrode configuration, electrode spacing, applied current, true earth resistivities, number of layers, layer thickness, potential gradient, and anisotropic earth properties. In the case of a homogeneous medium the measured apparent resistivity is equal to the actual or true resistivity. In some cases, the apparent resistivity, depending on how the above-mentioned parameters vary, may be a crude approximation of the

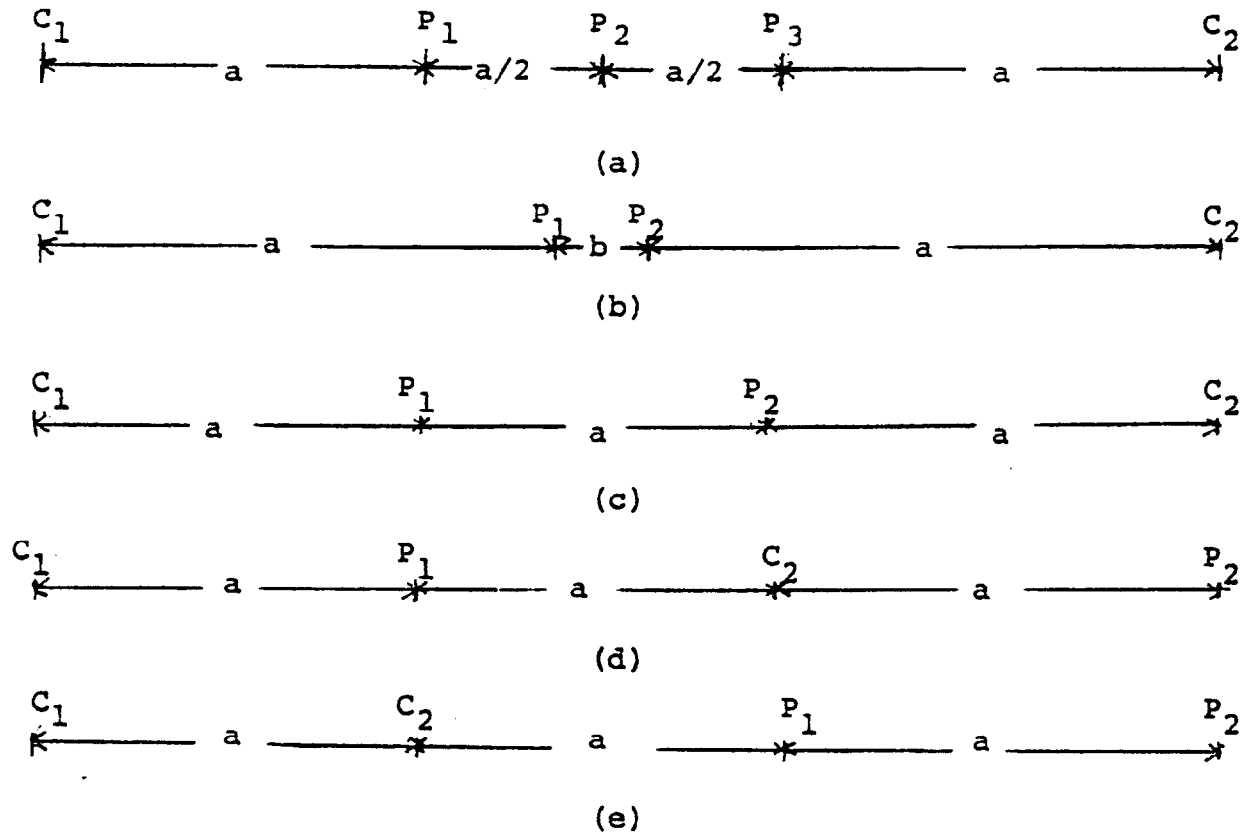


Figure 2: Shown are the (a) Lee array, (b) Schlumberger array, (c) Wenner or CPPC array, (d) CPCP array, (e) CCPP array.

Where C_1 and C_2 are current electrodes, P_1 , P_2 , and P_3 are potential electrodes, and a and b are electrode spacings.

true resistivities near the electrodes. It may be larger or smaller than any of the true resistivities or, depending on the electrode configuration, may even be negative.

ELECTRODE CONFIGURATIONS

Frank Wenner (1912) was the first person to establish a fixed system for the in-place electrical measurements of earth materials. In the United States this is one of the most common electrode configurations used for resistivity surveys. It is by no means the most accurate method available for delineating changes in the earth's electrical properties. This is because the potential difference is merely the line integral of the potential gradient from one potential electrode to the other; that is, the apparent resistivity is approximated by a function of the average gradient between the potential electrodes. Therefore, the closer the potential electrodes are together, the better variations in resistivity can be detected, since the gradient averaging process tends to subdue the small anomalous values of the gradient that would indicate variations in subsurface electrical properties. For this reason other electrode arrays may be used in an attempt to reduce the distance between the potential electrodes. One such electrode configuration is the Lee partitioning array.

The electrode configuration for the Lee partitioning array is illustrated in Figure 2a. This array is the same as the Wenner array except that an additional potential electrode is placed at the center of the array. This in effect allows the potential gradient to be averaged over a distance only one-half as long as for the Wenner array,

offering greater sensitivity to anomalies which allows closer definition of geologic boundaries.

Another method of resistivity survey that minimizes the distance between the potential electrodes is the Schlumberger type survey, illustrated in Figure 2b. This electrode configuration minimizes the distance between the potential electrodes to the point where variations in the gradient are recognizable. The two potential electrodes are placed symmetrically about the midpoint of the configuration and a distance (b) apart. This distance (b) is kept small enough so that the electric field between the electrodes can be considered constant. This is done by keeping (b) less than one-fifth the separation distance between the current electrodes. Usually in the field (b) is kept less than one-tenth the separation distance between the current electrodes. This enables small anomalies to be identified that could be completely averaged out when using a less sensitive array. The Schlumberger earth resistivity survey has another advantage over the other four electrode symmetrical arrays because in the depth sounding type of survey only two electrodes need be moved at any one time; this facilitates a more rapid depth survey.

The Logn array, mentioned earlier in the literature review section, is a non-symmetrical array. It is also known as the one-electrode configuration and is the asymmetrical form of the Schlumberger configuration. Like the Schlumberger configuration, this array measures changes in potential gradient. The electrode configuration for this array is shown in Figure 3.

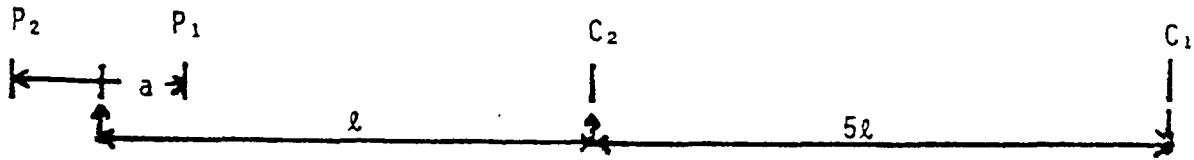


Figure 3: The Logn electrode configuration. P_1 and P_2 are potential electrodes, C_1 and C_2 are the current electrodes, (a) is the distance between potential electrodes, and (l) is the distance between the current electrode and the center of the potential electrodes.

The potential electrodes in this array are moved along the surface with a constant spacing (a) along lines passing through the single current source. The distance (a) between the potential electrodes is kept small as in the Schlumberger array to enable a precise gradient measurement. The second current electrode is placed at a distance of at least $5l$ away from the first current electrode, and usually is placed on the opposite side of the potential electrodes in the array. This second current electrode has no significant effect on the potential gradient measurement, since it is placed effectively at infinity with respect to the other elements. The apparent resistivity for this array is expressed by the function:

$$\rho_a = 2 \cdot \pi \cdot l^2 \cdot \Delta V / a \cdot I \quad (10)$$

where:

ρ_a = apparent resistivity

l = distance from current electrode

a = distance between potential electrodes

ΔV = potential gradient

I = current

The Logn electrode configuration was the configuration used by Bristow (1966) and Bates (1973) to locate subsurface cavities. Like the Schlumberger

configuration, this array has the advantage of moving only two electrodes at a time.

THE TRI-POTENTIAL ARRAYS

Given any four-electrode array with two current and two potential electrodes, there will be twenty-four ways in which these electrodes can be arranged. By subscript and letter designation these twenty-four arrangements all appear to be different, when in fact there are only three distinctly different arrays out of the possible twenty-four. These three arrays are illustrated in Figure 2c, d, and e. There are three reasons why this is so. For any given four-electrode arrangement, interchanging the subscripts of either the potential or current electrodes separately will alter the sign, but not the magnitude of either the resistance or the configuration factor. Changing the subscript of both the current and potential electrodes has no effect on either the configuration factor or the resistance. Disregarding sign, this leaves only six possibilities in which two current and two potential electrodes can be distributed. By use of the generalized form of the Helmholtz Reciprocal Relation, interchange of current and potential electrodes has no effect on the measured resistance, even in non-isotropic media (Searle, 1910); therefore, the twenty-four possible arrangements are reduced to just three different configurations.

The geometry factors (from Equation (6)) and the apparent resistivities (from Equation (5)) can be calculated for each of the

three electrode arrays. Apparent resistivities may be calculated by the expressions:

$$\rho_{\text{cppc}} = 2 \cdot a \cdot R_{\text{cppc}} \quad (11)$$

$$\rho_{\text{cpcp}} = 3 \cdot a \cdot R_{\text{cpcp}} \quad (12)$$

$$\rho_{\text{ccpp}} = 6 \cdot a \cdot R_{\text{ccpp}} \quad (13)$$

The resistance $R_{x_1 \times x_2 \times x_3 \times x_4}$ can be calculated by use of potential and current measurements. Let U_{ij} be the potential at electrode i due to current I entering the earth at electrode j . Then for the electrode arrangement $C_1P_1P_2C_2$ as illustrated in Figure 1 the resistance is given by:

$$R_{C_1P_1P_2C_2} = (U_{21} - U_{24} - U_{31} + U_{34}) / I \quad (14)$$

For the electrode arrangement $C_1C_2P_1P_2$, shown in Figure 4, the resistance is given by:

$$R_{C_1C_2P_1P_2} = (U_{41} - U_{24} - U_{31} + U_{32}) / I \quad (15)$$

For the electrode arrangement $C_1P_1C_2P_2$, illustrated in Figure 4, the resistance is given by:

$$R_{C_1P_1C_2P_2} = (U_{21} - U_{32} - U_{41} - U_{43}) / I \quad (16)$$

Equating Equations (14), (15), and (16), and applying the corollary to the Hemholtz Reciprocal Relation, one can relate the three resistance values by the formula:

$$R_{C_1P_1P_2C_2} = R_{C_1C_2P_1P_2} + R_{C_1P_1C_2P_2} \quad (17)$$

This implies that given any two of the resistances for two of the above electrode configurations, the third resistance can be calculated. This is an important concept that will be used later.

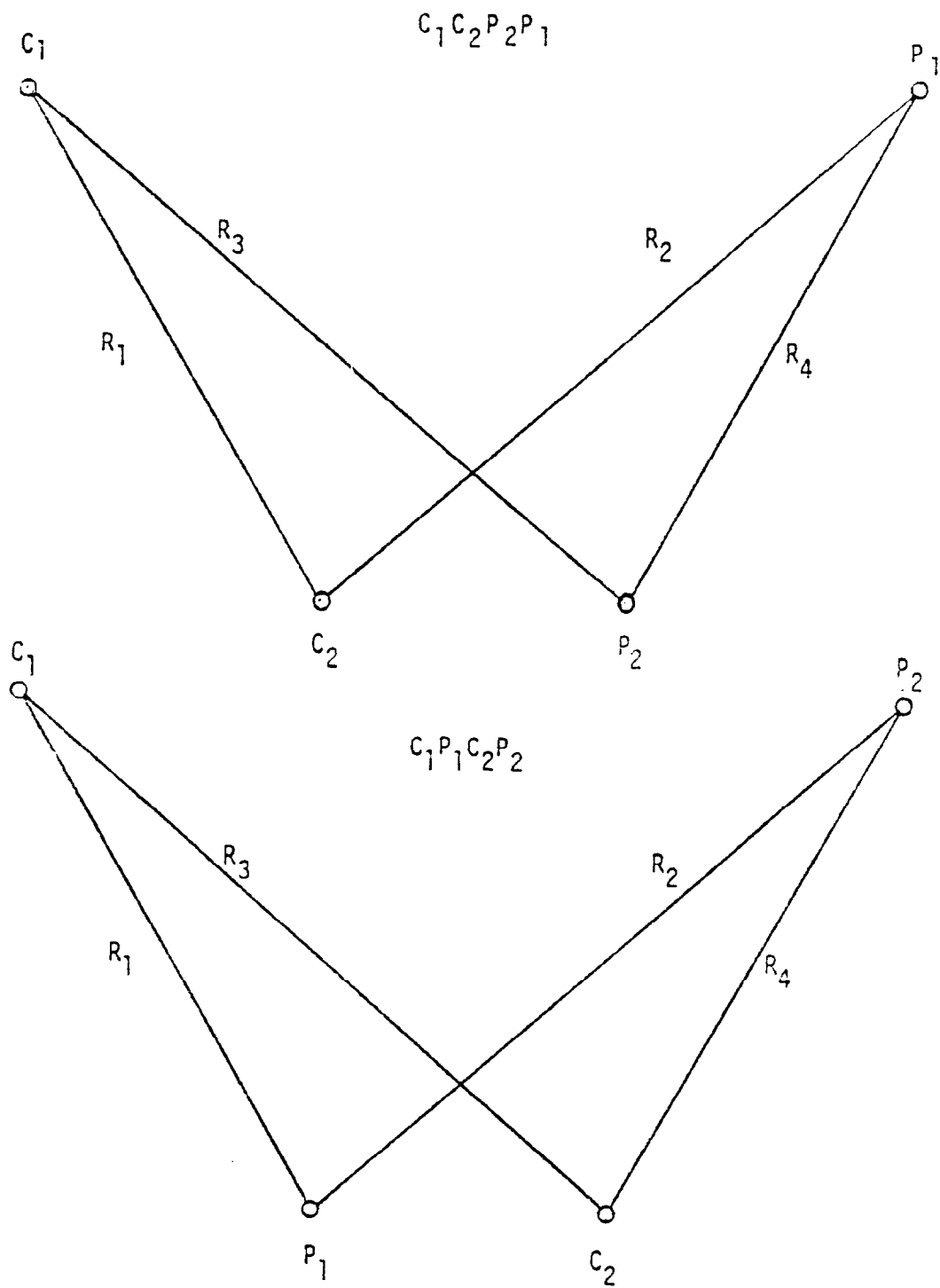


Figure 4: $C_1C_2P_1P_2$ and $C_1P_1C_2P_2$ electrode configurations where R_1 , R_2 , R_3 , and R_4 are distances.

FIELD TECHNIQUES AND THEORY

DEPTH SOUNDING TRI-POTENTIAL SURVEY

In the depth sounding tri-potential resistivity survey, the (a) spacing between electrodes is expanded and a plot of apparent resistivity versus electrode separation is obtained. In order to interpret the data, the assumption must be made that the resistivity of the underlying material varies as a function of depth only. In normal field practice, the validity of this assumption is usually not tested because of the large amount of time required. The tri-potential method of resistivity survey enables a rapid assessment of the validity of this assumption. This is because Equation (17) is true only if the above assumption holds for the field survey, such that:

$$\Delta = R_{c p p c} - R_{c c p p} - R_{c p c p} = 0 \pm \text{instrument error} \quad (18)$$

For this case, the resistances vary as a function of depth only. If this relationship does not hold, then lateral variations in resistance are in evidence. For this reason the tri-potential earth resistivity survey technique has a distinct advantage over the other forms of four electrode arrays used in the depth sounding surveys.

In this research the Δ (residual resistivity) value was divided by the CPPC resistance in an attempt to normalize the data. This new quantity is defined here as the $\Delta\%$ variable.

Typical uses for the depth sounding survey are next discussed. The primary use of the depth sounding survey is to delineate the nonindurated-indurated interface boundary. Usually there is enough of a resistivity contrast for this task to be accomplished. In some areas where there is a gradual change of resistivity with depth, this interface is

harder to locate. Examples of areas where this technique fails in delineating this interface are glaciated areas where clay-rich till overlies weathered shales. In this type of material, the resistivity contrast is not distinct, generally small and often non-existent, allowing no reliable determination of depth to bedrock. This is also a problem in areas containing a deep saprolite developed on metamorphic material, where the lower boundary of the saprolite is hard to define using the resistivity sounding survey.

The depth sounding survey is also used to delineate zones in unconsolidated sediments that show a relatively high resistance (500 to 2500 ohm-ft). These materials often show great potential as water producers since nonindurated sediments having high resistivities are usually sands and gravels. An illustration of using the tri-potential survey for water supply location is discussed under field results.

PROFILING TRI-POTENTIAL SURVEY

In the tri-potential profiling survey, the four electrodes are kept at a constant (a) spacing and moved in a line across the surface. In this way, a large area is covered at a relatively constant depth of investigation in a short time. This type of survey is basically concerned with locating anomalies associated with lateral variations in resistivities such as buried ore bodies, faults, fracture zones, cavities and filled sinks. The greater portion of work on resistivity surveying by Van Nostrand and Cook (1966) dealt with the profiling survey and theoretical curves for various electrode configurations; many hypothetical field cases are also discussed.

This research deals specifically with two types of problems using the tri-potential profiling survey. These are the location of fracture traces and the location of cavities and filled sinks. Locating fracture zones by the use of this technique will be discussed first.

Fracture Zones

In the field, a fracture can take on one of three resistivity distributions. These are the cases where the fracture is of a higher resistance than the parent rock, where the fracture is of a lower resistance than the parent bedrock and where there is no appreciable difference between the resistivities of the parent bedrock and the fracture. In the former two cases, the fracture will show up either as a peak or a trough in the profile plot of distance versus resistivity. Since only in the first two cases can the fracture be detected, only these two cases will be discussed.

The case in which the fracture resistivity is higher than in the surrounding rock generally occurs in areas where the parent rock is of a "low" resistivity (0-450 ohm-ft), and where the fluid in the porous zone along fractures is of a higher resistance than the surrounding rock. This can also occur in areas where the fracture zone has been cemented, for instance, by calcite cement; such cemented layers act as insulators when compared to the more conductive surrounding rock.

Theoretically, this situation can be modeled by use of a thin vertical insulating sheet in a conducting medium. This was done by Carpenter (1955). In this theoretical example, three cases were examined; these are:

- (i) the case in which all four electrodes are on one side of the insulating sheet,
- (ii) the case in which one of the electrodes is on the opposite side of the insulating sheet from the other three and
- (iii) the case in which two electrodes are on each side of the sheet.

For case (i), using image theory, Carpenter has shown that for the electrode arrangement $C_1P_1P_2C_2$ the apparent resistivity between the two potential electrodes can be expressed by the equation:

$$P_{a_{cppc-i}} = p\{1+1(2t+2)+1/(2t-2)-1/(2t+1)-1/(2t-1)\} \quad (19)$$

Similarly, for the $C_1C_2P_2P_1$ configuration,

$$P_{a_{ccpp-i}} = p\{1+3[1/t-1/(2t-1)-1/(2t+1)]\} \quad (20)$$

and for the electrode configuration $C_1P_1C_2P_2$,

$$P_{a_{cpcp-i}} = p\{1+3[1/(2t+2)+1/(2t-2)-1/t]\} \quad (21)$$

For case (ii), Carpenter has shown that for the electrode arrangement $C_1P_1P_2C_2$,

$$P_{a_{cppc-ii}} = p\{1/2+1/(2t+2)-1/(2t+1)\} \quad (22)$$

for the $C_1C_2P_2P_1$ arrangement,

$$P_{a_{ccpp-ii}} = p\{3/2+(3/2)t-3/(2t+1)\} \quad (23)$$

and for the electrode arrangement $C_1P_1C_2P_2$,

$$P_{a_{cpcp-ii}} = -3p\{1/2t-1/(2t+2)\}/2. \quad (24)$$

Note that in the last case, $p_{a_{cpcp-ii}}$ is negative.

For case (iii) and the electrode arrangement $C_1P_1P_2C_2$:

$$P_{a_{cppc-iii}} = p\{2+1/(2t+2)+1/(2-2t)\} \quad (25)$$

For the array $C_1C_2P_2P_1$, the current and potential electrodes are on opposite sides of the sheet and, therefore, the potential across the two potential electrodes is 0. For the $C_1P_1C_2P_2$ array:

$$\rho_{acpcp-iii} = p\{3+3[1/(2t+2)+1/(2-2t)]/2\} \quad (26)$$

where:

$$t = d/s$$

s = electrode spacing

d = distance between the center of the array and the insulating sheet

p = resistivity of surrounding media

From the above eight equations, one can plot apparent resistivity versus distance to obtain the theoretical plot of the resistivity distribution of transverses over a fracture for each of the three electrode arrays. Figure 5 shows the normalized plot of these relationships. As one can see, the curve is discontinuous at the critical points where the bounds of the equations representing these curves overlap. In actuality, this theoretical curve is not encountered in nature because the assumptions of nonconductance and infinitesimal thickness of the insulating sheet in the theoretical model are not met in the field. Therefore, the actual resistivity and the width of a fracture zone must be accounted for. The effect of resistivity contrast on the shape of the theoretical curve is shown in Figure 6 where the fracture is of a higher resistance than the surrounding rock, and in Figure 7 where the fracture is of a lower resistance than the surrounding rock. Figure 8 shows the effect of variations of fracture width on the resistivity profile for a constant resistivity contrast of +0.6.

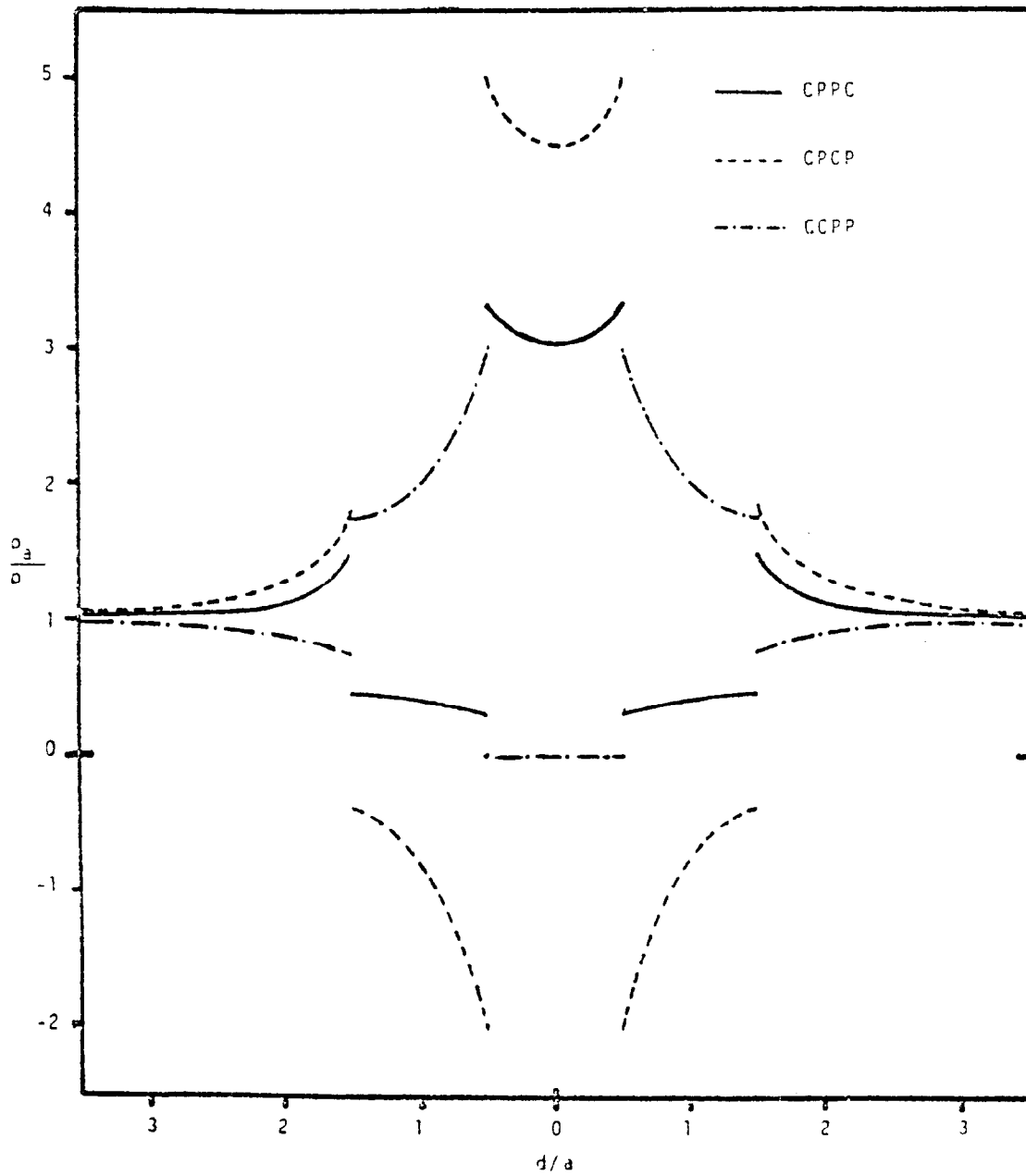


Figure 5: Theoretical tri-potential profile across a vertical infinite insulating plane.

d = distance, a = electrode spacing, p_a = apparent resistivity and p = background resistivity at infinity.

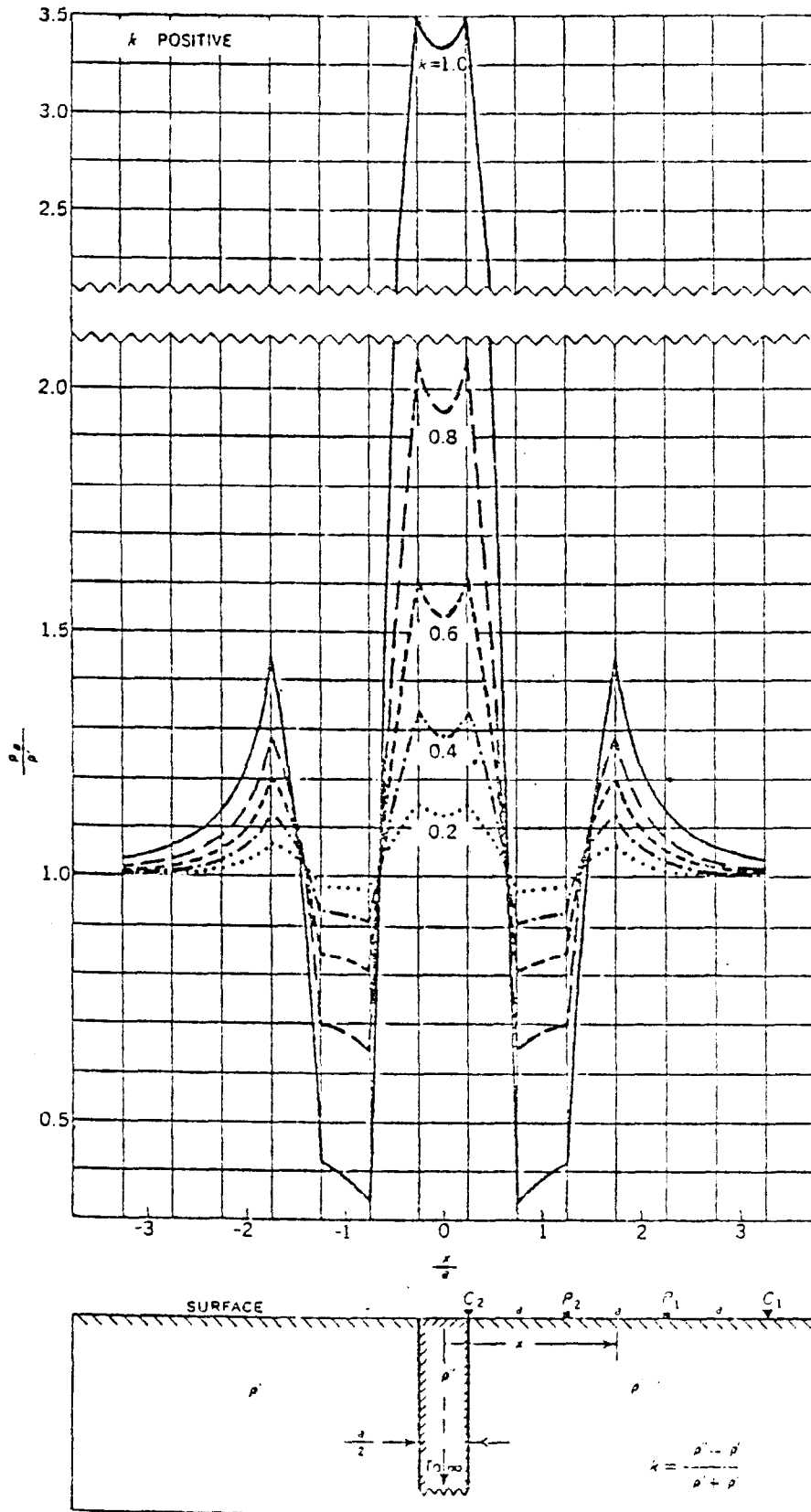


Figure 6: Effect of positive resistivity contrasts on anomaly associated with fracture trace using the CPPC array survey (Van Nostrand and Cook, 1966).

The fracture resistance exceeds the surrounding rock resistance and $k =$ resistivity contrast.

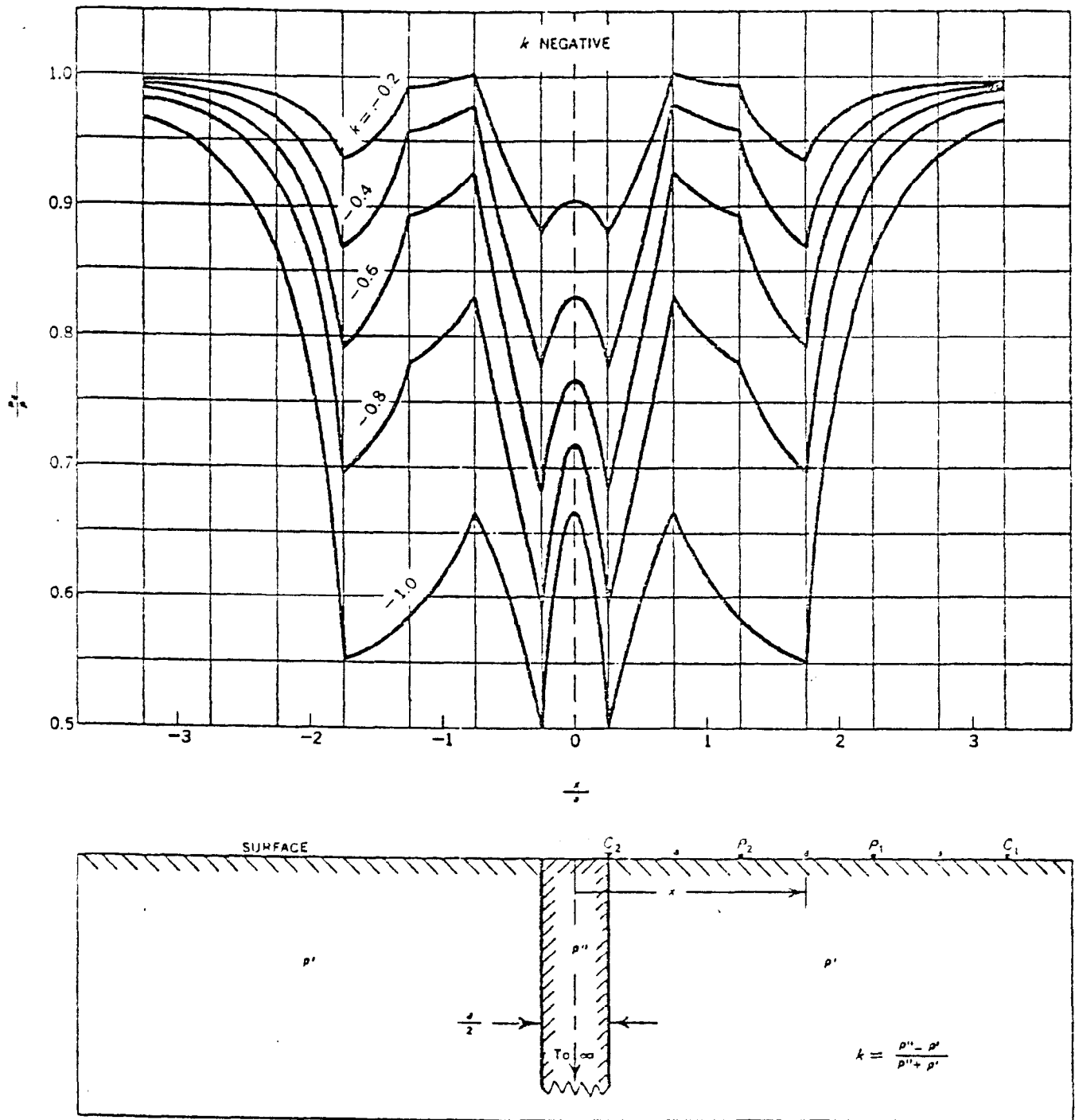


Figure 7: Effect of negative resistivity contrasts on anomaly associated with traverse across fracture zone using the CPPC survey (Van Nostrand and Cook, 1966).

Rock resistance exceeds fracture resistance and $k =$ resistivity contrast.

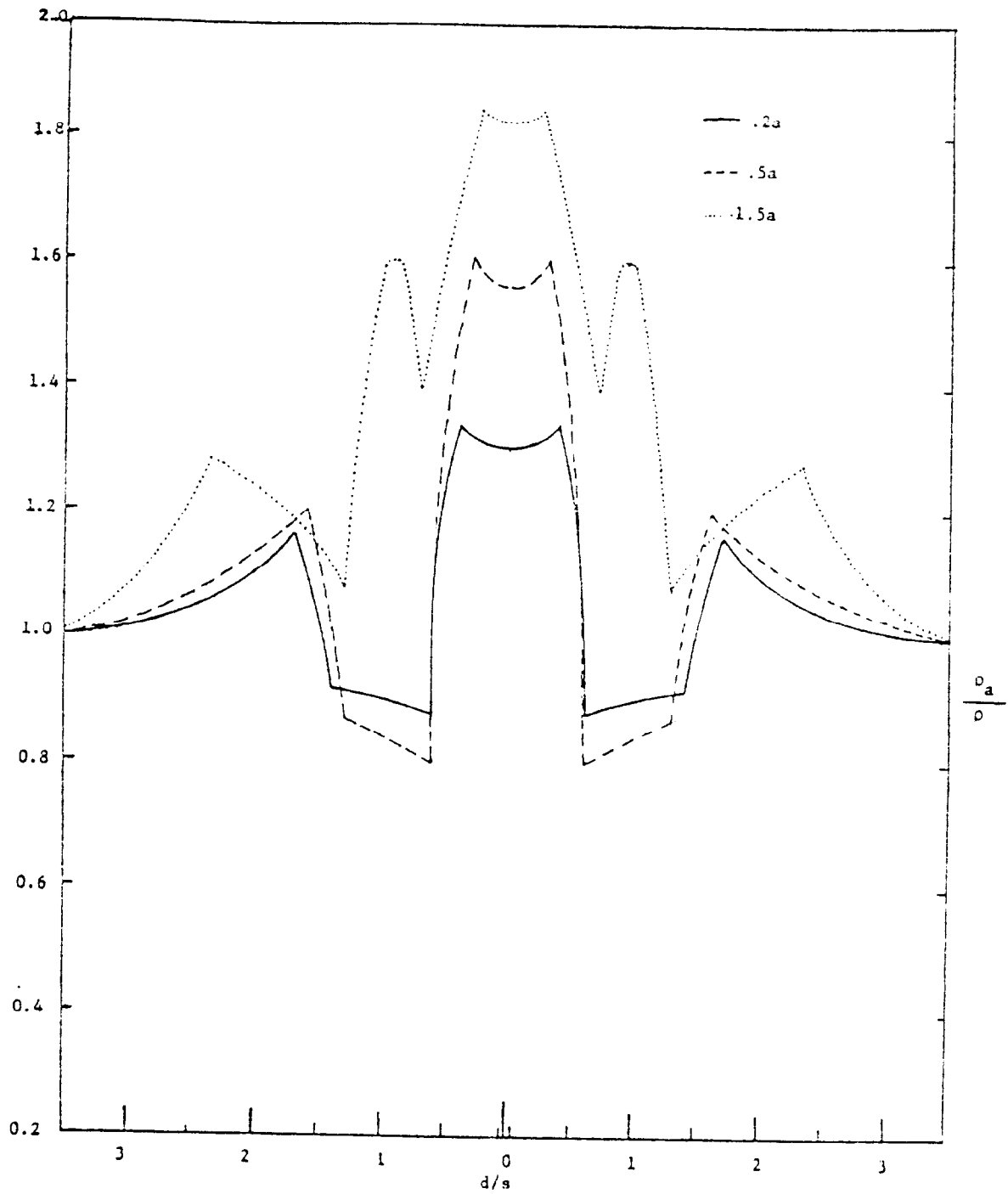


Figure 8: The effect of variations of fracture width on the resistivity profile for a constant resistivity contrast of +0.6 for cpc array. The three plots are for fracture widths of $0.2a$, $0.5a$ and $1.5a$, where (a) is the electrode spacing.

Another important variable is the (a) spacing, a variable that helps to define the resolution of the resistivity survey. Figure 9 illustrates how the (a) spacing affects the magnitude of the resistivity anomaly associated with the fracture zone and detected with the CPPC survey. It becomes apparent from this illustration that the smaller the (a) spacing, the larger the magnitude of the anomaly. Due to less than ideal situations when running the resistivity survey in the field, it is highly desirable to have a large anomaly associated with fracture zones. It is, therefore, desirable to minimize the (a) spacing whenever possible.

The point of diminishing returns, when decreasing the (l) spacing in surveys, is reached when one of two circumstances is met. One of these is when the (a) spacing becomes so small that the time involved to perform the profiling survey is prohibitive. The other situation occurs when the small (a) spacing does not allow the detection of bedrock or the fracture zone because of soil or nonindurated cover. In general practice, a depth sounding survey should be performed prior to the profiling survey to determine the depth to bedrock, in order to properly determine the most sensitive (a) spacing. From field experience, approximately 1.3 times the depth of the soil zone is probably an optimum (a) spacing. It should be noted that this is only a generalization and that in areas where the soil is highly conducting, greater electrode spacings are needed to discriminate against the soil layer.

Cavities

The mathematical theory behind the location of cavities has yet to be adequately solved and it is beyond the scope of this research to do so. A brine tank modeling experiment done by Habberjam (1969) using an insulating

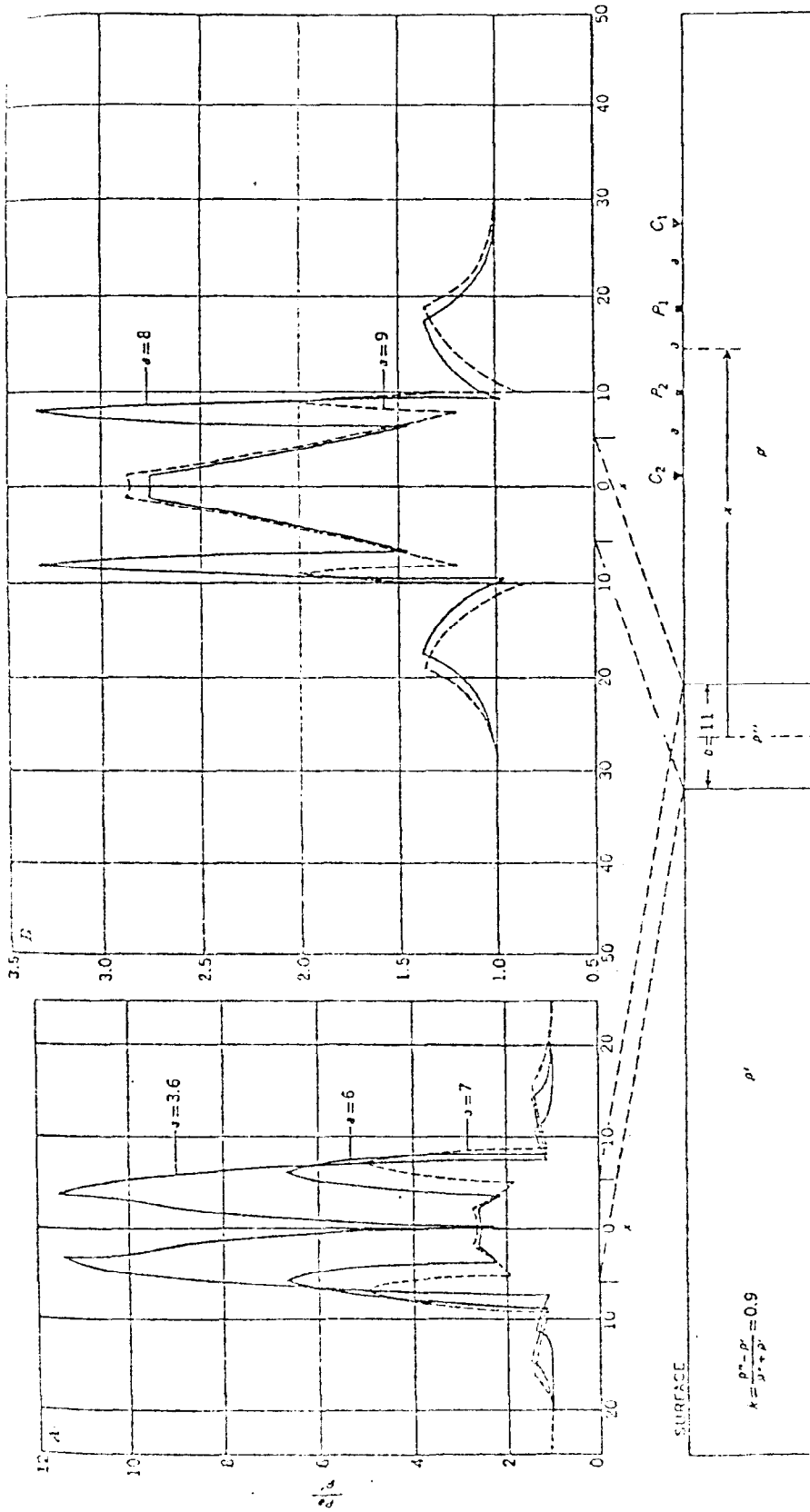


Figure 9: Effect of electrode separation on the resistivity profile across a vertical fracture zone (Van Nostrand and Cook, 1966), where a = electrode spacing.

sphere was one of the first attempts to delineate the theoretical curves for the tri-potential technique. The results of this research will be summarized here to better understand how the tri-potential technique will respond as one passes over a buried cavity with the profiling survey.

The shape of the theoretical curves obtained by traversing over the buried sphere are dependent on the electrode configuration used (CPPC, CPCP OR CCPP), on the ratio of depth of burial to the radius of the sphere and on the ratio of the electrode spacing to the sphere radius. In a homogeneous medium Equation (18) equals zero; therefore, only two of these electrode configurations were used in this modeling experiment. The theoretical response of the two surveys is illustrated in Figure 10. However, the field work associated with this research shows that the relationship mentioned above does not hold true as one passes over a buried cavity. Depending on survey conditions, the response of the CPPC resistivity survey, in fact, varied from that of a single peak to that of a triple peak, while the CPCP resistivity survey results varied from a double peak response to a triple peak response.

The brine tank modeling experiment of Habberjam (1969) shows that responses to the CPPC and CPCP surveys can be used to identify the values of h/r and a/r , which are respectively, depth to top of sphere divided by sphere radius and electrode spacing divided by the radius of the sphere. Since the electrode spacing (a) is always known, (h) and (r) can be determined. The two values that best show the effects of (h) and (r) are:

- a. The CPPC maximum ratio. This is the ratio of the peak apparent resistivity value (which in all cases occurs directly over the top of the buried

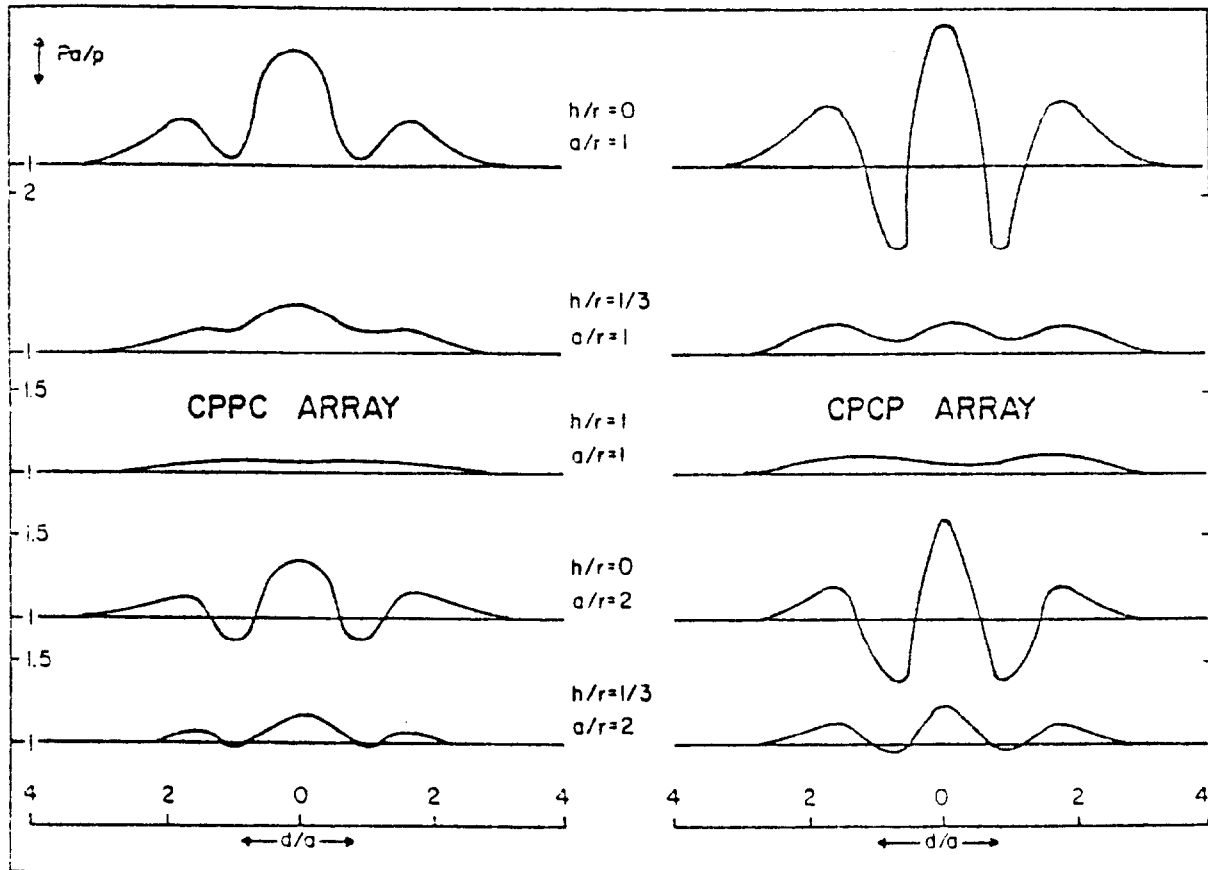


Figure 10: Tri-potential resistivity response to perfectly insulating sphere, from Habberjam (1969).

Where d = distance from center of sphere
 r = radius of sphere
 a = electrode spacing
 h = depth to top of sphere
 ρ_a = apparent resistivity
 ρ = resistivity of surrounding media

cavity) to the CPPC resistivity an infinite distance away from this cavity. This value is expressed as:

$$P_{\text{CPPC}_{\text{MAX}}} / P_{\text{CPPC}_{\infty}} = \alpha \quad (27)$$

- b. The CPCP fraction. This is the ratio of the mean value of the CPCP resistivity at a distance (d) from the central CPCP peak to the CPCP resistivity at infinity. This value is expressed as:

$$P_{\text{CPCP}_{\beta}} / P_{\text{CPCP}_{\infty}} = \beta \quad (28)$$

These values are plotted against h/r and a/r in Figure 11.

Within the observed range, each member of the α family of curves intersects all members of the β family of curves only once. These curve intersections result in unique points which correspond to unique values of h/r and a/r . Since (a) is always known, the depth and size of the spherical cavity can be determined. The limits for detection in this experiment are for a sphere of radius r buried to a depth r below the surface and a sphere with a radius of $a/5$ grazing the surface. When looking for caverns and deep mines these limits of detection would seem to preclude deeper investigations. However, this is not the case since caverns and deep mines are better approximated by cylinders and plates, rather than spheres. Larger anomalies would result from modeling these three-dimensional types. The field results do, in fact, show this to be the case. This conclusion is further substantiated by the work of Myers (1975). In this work he reviewed the various methods of resistivity surveying used up to that time in locating cavities.

He concluded that brine tank modeling was very valuable provided other shapes than spheres are used, since spheres do not accurately model the shape of most cavities as they occur in nature.

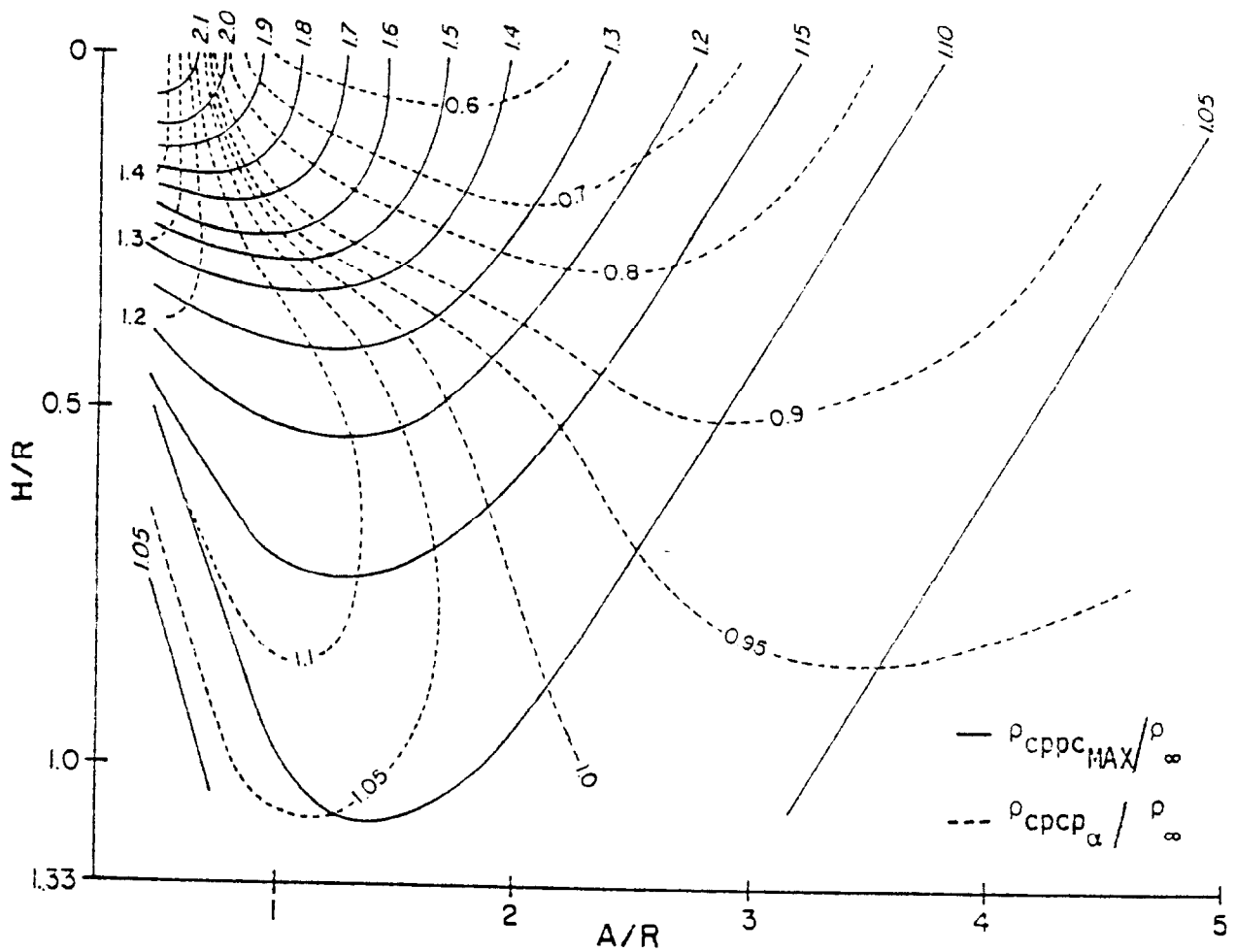


Figure 11: Chart relating $p_{cpcp_MAX} / p_{\infty}$ and $p_{cpcp_alpha} / p_{\infty}$ response to electrode spacing (a), sphere radius (r) and depth to top of sphere (H), Habberjam (1969).

FIELD RESULTS

The field work for this research project can be classified into the two general survey categories of profiling and depth sounding. At the underground coal gasification site in Wetzel County, the profiling surveys were used to locate fracture zones, while the depth sounding survey was used to evaluate the resistivities of stratigraphic units overlying the Pittsburgh coal seam. The results of the profiling surveys will be discussed first.

PROFILING TRI-POTENTIAL SURVEYS

The greatest bulk of field work was spent on the profiling surveys at the Underground Coal Gasification (UGC) site (see Figure 12) of the U.S. Energy Research and Development Administration (ERDA)--Morgantown Energy Research Center (MERC) in Wetzel County, West Virginia; this part of the research project involved locating previously unknown fracture zones as well as confirming the location of suspected fracture zones. Profiling surveys were initially run across areas that showed the most probable location of fracture zones through aerial photo-lineament analysis. In addition to these surveys, profiles were run to determine if there were any additional fracture zones that showed little or no surface expression and could, therefore, not be detected by aerial photo-analysis.

The resistivities typically encountered at the UGC site were in the range of 90 to 300 ohm-ft, and were predominantly below 200 ohm-ft. This is consistent with the rock types at or near the surface. At the UGC site the soils are clay-rich, formed from grey acid shales and fine-grained dirty sandstones. The resistivity range encountered at the UGC site, therefore, seems to be realistic for this terrain.

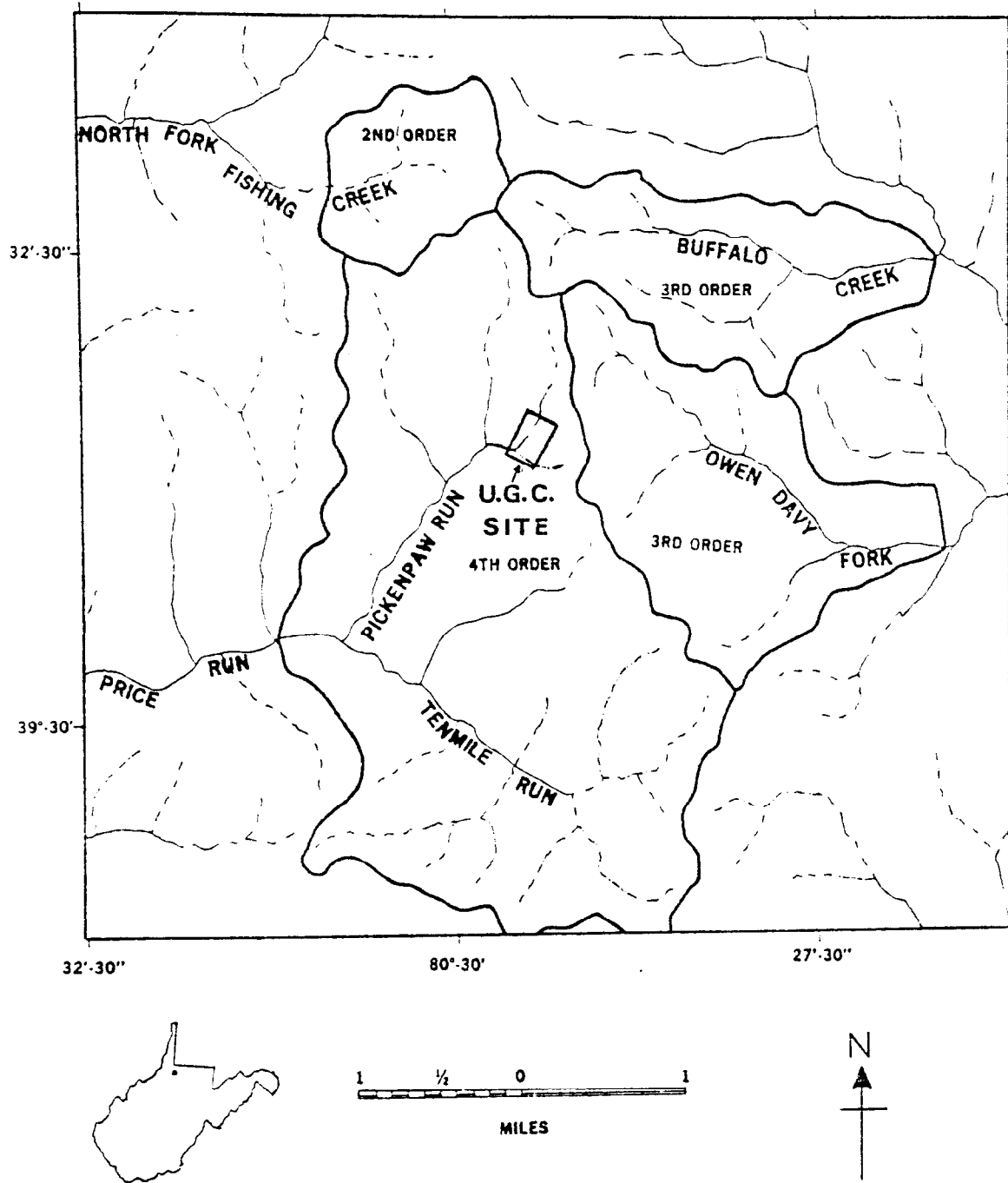


Figure 12: Outline of Drainage Basins containing the Underground Coal Gasification (U.G.C.) site, modified after Sole et al. (1976).

For each traverse at this site two electrode spacings were utilized: a 10 ft spacing and a 40 ft spacing. The 10 ft spacing was chosen because it was believed that this would be the minimum electrode spacing required to detect fractures below the typically 2 to 4 ft thick, highly conducting soil zone. The 40 ft spacing was chosen because it was estimated that anything longer would be unmanageable in the heavily vegetated areas where a number of the surveys were run.

This site had been logged approximately 40 years ago and, therefore, the old abandoned logging roads that ran parallel to the hill contours were used for three of the profile lines. The remainder of the profiles were run in the valley bottom areas of the site that had been used as pasture for many years. Approximately two weeks were required to clear the old logging roads and portions of the valley before the resistivity profiles could be run. The last part of July and the entire month of August, 1974, were required to gather this data. All of this field data was collected using a Soil Test model R-40 Terra Scout resistivity meter that had been modified by the installation of a switching circuit to facilitate the rapid change from one electrode array to another.

A map of the location of these traverses is shown in Figure 13, which also shows the location of the fracture zones found by the tri-potential surveying. The most prominent photo-lineaments in the study area occur along the two fracture zones bearing 115° and 37° . These are drainage or stream photo-lineaments, which also show up especially well on 1.5-1.6 millimicron multispectral scanning imagery. The two pairs of fracture zones bearing 104° and 106° are not associated with photo-lineaments previously mapped by the Morgantown Energy Research Center, with one exception: a photo-lineament

detected on high-altitude color infrared photography falls along the northernmost fracture zone bearing 104° , and is possibly associated with both fracture zones with this bearing. On the other hand, most mapped photo-lineaments at the UGC site are not associated with near-surface resistivity anomalies.

Figure 14 shows the data from part of the resistivity profile H-H', as located on Figure 13. This survey was done along an old logging road high on the hill to the east of the UGC site. Figure 14 shows the response of the resistivity profiling survey as the array passes across two shallow fracture zones bearing 104° along the northern half of survey H-H'. It can be seen that the 10 ft electrode spacing had a greater response than the 40 ft spacing. The maximum response for the 10 ft spacing is 2.4 times the background resistivity for the CPCP array. For the same array at the 40 ft spacing, a maximum of 1.7 times the background resistivity is reached. As one passes over the second fracture zone, the 10 ft CPCP response resistivity factor is 1.9 while the 40 ft CPCP response factor is only 1.2. The resistivity values for the second fracture alone indicate that the resistivity anomaly associated with this fracture zone does not extend at depth since the 40 ft spacing response is much less than the 10 ft spacing response. This is confirmed by the delta percent values ($\Delta\%$) for the 40 ft (a) spacing. As the 40 ft spacing survey passes over both fracture zones, there is little response in the $\Delta\%$ value, while the 10 ft spacing survey shows a large response in this value. This further indicates that these anomalies extend only to a shallow depth. Similar responses were obtained as one passed over the fractures along traverse H-H' that are to the south-southwest of the first two fracture zones. In addition, similar responses were observed when passing across these four shallow fracture zones along the traverses J-J', G-G' and D-D'.

A different type of response was noted in traverses C-C' and D-D' as one passed over the fracture bearing 115° (shown in Figure 15) that seems to be associated with one of the valleys that is present at the UGC site. A much larger response is evident from this figure than in Figure 14. The 10 ft (a) spacing survey reaches a maximum value of 3.2 times the background resistivity. This response is over a wider area than the previously mentioned fracture zones. The 40 ft (a) spacing also shows a large response to this anomaly. This indicates that the 115° fracture is deeper and wider than the fractures bearing 104° and 106°.

Both the 10 ft and the 40 ft $\Delta\%$ values show maximum responses much greater than the background $\Delta\%$ values, indicating again that the resistivity anomaly associated with the fracture extends to a depth greater than the other fractures. From these large $\Delta\%$ values one can conclude that the 115° fracture zone may well extend down to several hundred feet. No definite determination of the depth can be made since only two (a) spacing surveys were run across the fracture zone. The 10 ft $\Delta\%$ plot is of particular interest since it responds at two points along the traverse. Theoretically this type of response would result as one passes across a vertical resistivity boundary or zone. Data analysis shows that this fracture zone is approximately 50 ft wide as indicated by the distance between the two maximum points for the 10 ft spacing $\Delta\%$ traverse. A similar response was obtained as traverse C-C' passed across the fracture bearing 115°.

The fracture bearing 37° has a somewhat varied resistivity response associated with it. The largest response was obtained along traverse B-B', while the least response occurred on traverse F-F'. The least response is probably because of the small angles with which this traverse intersects the fracture zone. Traverses A-A' and B-B' showed responses for the 37° fracture

which were similar to, but of a smaller magnitude than those associated with the fracture bearing 115° . These two traverses indicate that the peaks in the $\Delta\%$ traverse for the 10 ft electrode spacing are between 20 and 30 ft apart, indicating that the 37° fracture is about 25 ft wide at this point. Traverses C-C', E-E' and F-F' show a single peak for both the resistivity values and $\Delta\%$ values as this fracture was encountered; therefore, no width estimate can be made at these points. Also, at the three points where these traverses pass across the 37° fracture, the 40 ft $\Delta\%$ values are only about one-fourth of those associated with the fracture bearing 115° , indicating that the anomaly associated with the 37° fracture is shallower than that for the 115° fracture.

A pilot study was also undertaken to determine the feasibility of using the tri-potential technique for locating underground coal mines. A profiling survey using the Soil Test Terra Scout resistivity meter was run over a 200 ft deep coal mine in the Pittsburgh Coal seam near the Morgantown Municipal Airport. This survey was successful in detecting the presence of the mine at that depth. However, it is doubtful if resistivity surveying techniques can locate coal mines much deeper than this.

DEPTH SOUNDING SURVEY

A large-scale depth sounding survey was performed at the U.S. ERDA-MERC UGC site in Wetzell County, West Virginia; the purpose of this survey was to evaluate the apparent resistivities of the Pittsburgh Coal seam and overlying stratigraphic units before initiation of coal burning at the UGC site. Originally another survey was to have been run during the coal burning phase of the UGC project for comparison with the initial depth sounding survey.

However, the second survey was not possible because of lengthy delays in the initiation of the burn (which did not take place as of September, 1976).

Several preliminary depth sounding surveys were run before the large-scale survey, using either a Soil Test Terra Scout or a Bison model 2350 resistivity meter. The maximum depth of investigation under ideal conditions for the Soil Test Terra Scout is 200 ft and for the Bison model 2350 is 400 ft. Neither of these instruments then have sufficient capabilities to accurately determine the apparent resistivity for electrode spacings larger than 400 ft.

The instrument that was used for the large-scale depth sounding survey was one developed at the U.S. ERDA, Denver Mining Research Center by Lepper and Scott (1974). The design and operation of this instrument is described in detail by Lepper and Scott (1974). This instrument has the disadvantage that a simple null is not used to determine the earth resistance; an oscillating null is instead used. In order to obtain a reading, one has to minimize the back-and-forth oscillating motion of the null meter. At small electrode spacings where the signal-to-noise ratio is high, this is a simple task. At large electrode spacings where the signal to noise ratio is low, even at the optimum null the oscillations are very high. This large oscillation amplitude makes it difficult to determine just where the optimum null position is. In this particular instrument, another disadvantage was that instead of a solid state relay, a mercury relay is used to obtain the low frequency square-waved current output. This mercury relay cannot handle the rapid switching necessary for any length of time. As a result of this, the relay had to be replaced approximately six times during the course of the

survey. This resulted in much wasted time while relays were sent back and forth between West Virginia and Colorado; this necessitated that the survey be conducted over a several-month period.

There were three test holes drilled at this site, as shown on Figure 13. Gamma-ray, caliper, and induction logs were obtained for these test holes. The induction log was used to determine the actual resistivity of each layer so that a comparison could be made with the apparent resistivities obtained with the tri-potential depth sounding survey. The resistivities obtained from the induction log are plotted on Figure 16 as bar graph values versus depth. Also plotted on Figure 16 are the tri-potential apparent resistivities and tri-potential residual resistivity versus electrode spacing. The scales for depth and electrode spacing are the same on this figure. It must be noted here that the electrode spacing is not the same as the depth of investigation, as is sometimes the case when a simpler layered situation is studied.

The apparent resistivity data for this survey is plotted in Figure 16. These data appear to approximate one of the classic forms of the four layer case, where the first layer resistivity is higher than the second layer; the second layer resistivity is lower than the third layer and the third layer resistivity is higher than the fourth. Using standard curve fitting techniques (Bhattachary and Patra; 1968), one solution to this layered distribution is:

$$\begin{array}{ll} \rho_1 = 1000 \text{ ohm-ft} & Z_1 = 12 \text{ ft} \\ \rho_2 = 200 \text{ ohm-ft} & Z_2 = 50 \text{ ft} \\ \rho_3 = 900 \text{ ohm-ft} & Z_3 = 400 \text{ ft} \\ \rho_4 = 300 \text{ ohm-ft} & Z_4 = \infty \end{array}$$

where ρ , apparent resistivity and Z is the depth to a layer's bottom for layers 1 (uppermost), 2, 3, and 4. This is a much more simplified system

than actually is occurring in the field and represents averages of the true resistivities of the actual formations in the field.

The geophysical logging performed by the MERC started at a depth of 70 ft below the surface. The values of formation resistivity as determined by the induction log are plotted in Figure 16 along with the surface survey data. In almost all cases the apparent resistivity determined from the tri-potential depth sounding survey is greater than the formation resistivity as determined by the induction log for a corresponding depth and electrode spacing. This is another example illustrating the inaccuracy of the general rule of thumb which assumes the electrode spacing is equal to the depth of investigation. This is especially true in clay-rich soils and conductive formations such as those that occur at this site. In highly conductive materials it is often necessary to have an electrode spacing three times larger than the depth of investigation.

The residual $\Delta\%$ values for this survey show that lateral variations in resistivity apparently affect the data at various points along the survey. These affected points correspond to resistivity data for:

8 -	14 ft	electrode	spacing
24 -	48 ft	"	"
70 -	80 ft	"	"
130 -	140 ft	"	"
350 -	400 ft	"	"
550 -	800 ft	"	"
1000 -	1500 ft	"	"

As mentioned earlier, when the electrode spacing increased, so did the difficulty with which the instrument was read. This may well account for the

erratic nature of the data for electrode spacings greater than approximately 150 ft. Thus the $\Delta\%$ may not be reflecting variations in resistivity at all for these greater depths. Due to equipment limitations at the present, it is not possible to use the UGC data to establish the greatest depths to which a tri-potential depth sounding survey could give estimates of resistivities in this area.

RESISTIVITY MODELING

A computer model was constructed for simulating the results of a depth sounding survey for the tri-potential technique, to determine the reliability and sensitivity of the tri-potential depth sounding survey used at the UGC site in this study. The computer program was designed after Mooney, et al. (1966), with the help of Dr. Roy Greenfield of the Pennsylvania State University. This program was then modified by the senior author. A copy of this program appears in Appendix A.

The input data to the computer program consisted of corrected and averaged resistivities for strata obtained from induction logs, thicknesses of combined stratigraphic units from induction logs, and several hypothetical electrode spacings. The program output consisted of resistivity contrasts for each set of adjacent stratigraphic units, and predicted apparent resistivities for various electrode spacings. A calcomp plotter then was used to plot predicted apparent resistivity versus electrode spacing.

Induction log data used in the computer program was not available for the upper 70 feet of strata; the measured resistivity for the first layer encountered (99 ohm-ft) was therefore used as the average resistivity for the upper 70 feet layer. Induction 109 data was reduced to give the average resistivities for 24 defined layers, situated between the ground surface and the Pittsburgh Coal seam. These data were then utilized by the computer program.

Figure 17 shows plots of the modeled apparent resistivities (from the program) versus electrode spacing as well as the apparent field resistivities (from the tri-potential depth sounding survey) versus electrode spacing. This figure shows that the tri-potential apparent resistivity and the computer modeled apparent resistivity trends are initially divergent, but start to converge with increased electrode spacing, starting at approximately a 30 ft. spacing. For greater electrode spacings the two resistivity trends are approximately parallel to each other, with the tri-potential trend being higher. This indicates that the apparent resistivity data from the tri-potential field survey do respond as theoretically predicted by the modeled apparent resistivity data. Many of the differences between the two resistivity trends of Figure 17 are probably caused by error in the assumed average resistivity for the upper 70 feet of ground, and hence by error in the computer model. In addition, the computer program was used to resolve the apparent resistivity data obtained from the tri-potential survey into true average resistivities versus depth for four combined stratigraphic units. The results are identical to those obtained using the standard curve fitting techniques, as previously presented in this report.

CONCLUSIONS

GENERAL CONCLUSIONS

This research project has shown that the tri-potential method of resistivity survey can be used in many applications and is an improvement over other resistivity survey methods, because:

1. Additional data can be obtained with the tri-potential survey with little additional investment of time over the Wenner array survey, since the three electrode tri-potential arrays can be obtained by the flip of a switch and not the physical moving of electrodes.
2. Depending on the situation, the CPCP or CCPP apparent resistivities are more responsive to variations in resistivity distributions in the subsurface than the more common CPPC (Wenner) apparent resistivity. This often allows one to distinguish between smaller variations in resistivity than would be possible using just the CPPC array.
3. The degree of lateral variation in resistivity can be determined in order to assess the validity of the depth sounding interpretation method by the use of the $\Delta\%$ variable. This method is only accurate if there are small lateral changes in resistivity.
4. In the horizontal profiling survey, the tri-potential $\Delta\%$ residual variable is useful in identifying the type of anomaly and helps to give an estimate of the depth to the anomaly.
5. The tri-potential profiling technique can be used to substantiate lineament analysis from photographs to determine if fracture zones are associated with these lineaments; it shows successful results

in locating fracture zones. The nature of anomalies associated with fracture traces compare favorably with theoretical predictions.

6. The depth and sometimes the width of a fracture zone can be assessed by an examination of the $\Delta\%$ value for various electrode spacings of the profiling survey.

7. The tri-potential resistivity surveying technique is capable of detecting and locating deep coal mines down to a depth of at least 200 ft, but probably not much deeper. A more promising geophysical surveying technique for locating deep mines is shallow reflection seismic surveying; this technique is recommended for future use in locating and mapping general areas underlain by poorly-known coal mines.

CONCLUSIONS FOR UGC SITE

1. The horizontal profiling survey using the tri-potential technique was useful for locating fracture zones at the UGC site, as well as for determining their approximate width at the ground surface.

2. The approximate depth of fracture zones at the UGC site can be determined by the tri-potential technique if a powerful enough resistivity unit is used together with several profiling surveys having different electrode spacings.

3. Some detected fracture zones are associated with photo-lineaments, but most photo-lineaments apparently do not correspond to fracture zones at the UGC site. The two most prominent fracture zones are overlaid by the most prominent photo-lineaments in this area.

4. Computer modeling of apparent resistivity versus electrode spacing has shown that the tri-potential depth sounding technique gives reasonably reliable estimates of apparent resistivity as a function of electrode spacing at the UGC site.

5. The Leeper and Scott resistivity meter was not sensitive enough to resolve the different resistivities of thin layers at the UGC site, using depth sounding tri-potential surveys. Moreover, it is doubtful that the tri-potential method or any other resistivity survey method could adequately detect differences in the apparent resistivities of thin rock layers at the UGC site or elsewhere.

6. The tri-potential depth sounding technique (as well as other resistivity surveying methods) will probably not be useful in detecting the burn front in the Pittsburgh Coal seam at the UGC site, after burning begins. This technique is probably not sensitive enough to detect resistivity changes in a coal seam at such a great depth (about 900 feet).

7. The induced polarization technique as well as shallow reflection seismic surveying would most likely prove useful in detecting and monitoring the burn front during future burning of coal underground, both at the UGC site and elsewhere.

SELECTED REFERENCES

- Arandjelovic, D., (1965) *Conditions for the Application of Resistivity Methods in the Karst Area of the Trebisnjica Hydro-system*, Zavod Geol. i. Geofiz. Intraziuanja Vesnik Primen Geofizika. ser. C. nos. 4-5, pp. 185-208.
- Bates, E. R., (1973) *Detection of Subsurface Cavities*, U.S. Army Corps of Engineers, Misc. Paper S-73-40, Vicksburg, Mississippi.
- Bhattachary, P. K. and Patra, H. P., (1968) *Direct Current Geoelectric Sounding*, Elsevier Pub. Co., New York.
- Bristow, C., (1966) *A New Geophysical Resistivity Technique for Detecting Air-Filled Cavities*, Studies in Speleology, Vol. 1, Part 4, pp. 204-227.
- Buhle, M. B., (1953) *Earth Resistivity in Ground Water Studies in Illinois*, Am. Inst. Mining Metall. Engineering Transactions, Vol. 196, pp. 395-399.
- Carpenter, E. W., (1955) *Some Notes Concerning the Wenner Configuration*, Geophysics Prosp., Vol. 3, pp. 388-402.
- Carpenter, E. W. and Habberjam, G. M., (1955) *A Tri-potential Method of Resistivity Prospecting*, Geophysics, Vol. 21, pp. 445-469.
- Day, J. G., (1964) *Cave Detection by Geoelectric Methods, Part 1, Resistivity*, Cave Notes Vol. 7 No. 3, pp. 17-22.
- Dobrin, M. B., (1960) *Introduction to Geophysical Prospecting*, McGraw Hill Book Co., New York.
- Dutta, N. P.; Bose, R. N.; Saika, B. C., (1970) *Detection of Solution Channels in Limestone Using Electrical Resistivity Methods*, Geophy. Prosp., Vol. 18 No. 3, pp. 405-414.
- Ebau, W. F., (1973) *Temperature Patterns in Soil Above Caves and Fractures in Bedrock*, Unpublished Master's Thesis, Penn. State University.
- Enslin, J. F., (1953) *Geophysics as an Aid to Foundation Engineering*, South African Inst. Civil Engineers Trans., Vol. 3, No. 2, pp. 49-60.

- Flathe, H., (1963) *Five Layer Master Curves for Locating the Salt-water-Freshwater Interface by Resistivity Methods*, Geophysics, Vol. 24, pp. 420-443.
- Flathe, H. (1964) *Investigation of Saltwater Intrusion by Use of Resistivity Sounding*, Geoph. Prosp., Vol. 17, pp. 340-357.
- Flathe, H., (1967) *Interpretation of Geoelectric Resistivity Measurements for Solving Hydrogeological Problems*, Mining and Ground Water Geophysics, Economic Geol. Rept. No. 26, Geol. Survey, Canada.
- Foster, J. W. and Buhle, M. B., (1951) *An Integrated Geophysical and Geological Investigation of Aquifers in Glacial Drift in Urbana, Illinois*, Econ. Geology, Vol. 46, pp. 367-397.
- Habberjam, G. M., (1969) *The Location of Spherical Cavities Using a Tri-potential Resistivity Technique*, Geophy., Vol. 34 No. 5, pp. 780-784.
- _____ (1970) *The Association of Resistivity Soundings*, Geophys. Pros. (Netherlands), Vol. 18 No. 2, pp. 199-214.
- HRB-Singer Inc., (1971) *Detection of Abandoned Underground Coal Mines by Geophysical Methods*, EPA Water Pollution Control Research Series 140.0 EHN 04/71.
- Kirk, G. K., (1976) *Evaluation of the Tri-Potential Resistivity Technique in Locating Cavities, Fracture Zones, and Aquifers*, Unpublished Masters Thesis, West Virginia University.
- Lepper, M. C. and Scott, J. H., (1974) *Improved Electrical Resistivity Field System for Shallow Earth Measurements*, U.S.B.M. Report RI 7942.
- Merkel and Kaminski (1972) *The Use of the Buried Electrode Resistivity Technique in Locating Fracture Zones*, Ground Water, Vol. 4, pp. 47-53.
- Mooney, H. M., Orell and E. Prickett, H. and Tornheim L., (1966) *A Resistivity Computation Method for Layered Earth Models*, Geophysics Vol. 31, pp. 222-231.
- Myer, J. O., (1975) *Cave Location by Electric Resistivity Measurements, Some Misconceptions and Practical Limits of Detection*, Trans. British Cave Research Assoc., Vol. 2 No. 4.

- Palmer, L. S., (1954) *Location of Subterranean Cavities by Geo-electric Methods*, Mining Mag., Vol. 91 No. 3, pp. 137-141.
- Searle, G. F. C., (1910) *On Resistances with Current and Potential Terminals* Electrician, Vol. 66 No. 25, pp. 999-1002.
- Sole, T. L., Byrer, C. W., Rauch, H. W., and Overbey, W. K. Jr., (1976) *Hydrogeologic Assessment of an Underground Coal Gasification Project Site, Grant District, Wetzel County, West Virginia*, ERDA Technical Progress Report-76/5.
- Stahl, R. L., (1973) *Detection and Delineation of Faults by Surface Resistivity Measurements*, Bu Mines RI 7824, 28 pages.
- Stahl, R. L., (1974) *Detection and Delineation of Faults by Surface Resistivity Measurements at Schwartzwalder Mine, Jefferson County, Colorado*, Bu Mines RI 7975, 27 pages.
- Van Nostrand, R. G., (1953) *Limitations on Resistivity Methods as Inferred From the Buried Sphere Problem*, Geophysics, Vol. 13 No. 423.
- Van Nostrand, R. G. and Cook, K. L., (1966) *Interpretation of Resistivity Data*, Prof. Paper 499, U. S. Geological Survey, Washington, D.C.
- Wenner, F., (1912) *The Four Terminal Conductor and The Thomson Bridge*, U. S. Bureau of Standards Bulletin, Vol. 8, pp. 559-660.
- Zohdy, J. M., Eaton, H., and Mabey, W., (1974) *An Integrated Study of the Ground Supply Potential Near Urbana, Illinois*, Illinois Geological Survey Water Resources Paper W-56 pp 63.

APPENDIX A

A Computer Program for Modeling Apparent
Resistivity as a Function of Electrode Spacing for
the Tri-Potential Survey

PAGE 0001 HEWLETT-PACKARD 32102A,01.1 FORIPAN WED, AUG 25, 1976, 11:13 AM

```

00001000 $CONTROL INIT
00001100 C    NTD(1)=DEPTH TO TOP OF I+1 LAYER
00001200 C    NL=#OF LAYERS
00001300 C    NT(N)=LAYER THICKNESS
00001400 C    NR(N)=LAYER RESISTIVITIES
00001500 C    CK(N)=RESISTIVITIES CONTRASTS
00001600 C    SP(N)=ELECTRODE SPACINGS
00001700 C    ISP=#OF ELECTRODE SPACINGS
00001800 C    LA=ARRAY CONFIGURATION
00001900 C    1=SCHLUMBERGER
00001910 C    2=WENNER
00001920 C    3=HALF WENNER
00001930 C    4=DIPOLE DIPOLE
00001940 C    5=POTENTIAL FUNCTION FOR ISOLATED CURRENT SOURCE
00001950 C    THIS PROGRAM WILL GENERATE THE APPARENT RESISTIVITY
00001960 C    CURVES FOR AN N LAYERED STRUCTURE N=1 TO INFINITY WITH
00001970 C    FINITE RESISTIVITY CONTRASTS E.G. NO PERFECTLY CONDUCT
00001980 C    ING OR INSULATING LAYERS.
00002000 C    DIMENSION NT(100),NR(100),NTD(100)
00003000 REAL CK(100),Q(2001),P(2,2001),M(2,2001),SP(100),SPC(100)
00004000 &,OK(2001),SCH(100),FSCH(100),AER(10),ERR(10),STOR,FEN(100),
00005000 &,WENNER(100),FENNER(100),SAVSP(100),FRES(100),FSP(100)
00005001 CHARACTER*10 MLESS1
00005002 INTEGER I,MLESS(5)
00005003 EQUIVALENCE(MLESS1,MLESS)
00005004 CHARACTER*20 RES1
00005005 INTEGER IRES(10)
00005006 EQUIVALENCE(RES1,IRE5)
00005007 CHARACTER CMD3*72
00005010 CHARACTER CMD4*72
00005011 INTEGER I,BUFF(500)
00005012 DATA MLESS1,RES1/MC-SPACINGS,,"APPARENT RESISTIVITY"/
00005020 DATA CMD4/"FILE F104=L:DEVELP;CCTL"/
00005021 DATA CMD3/"FILE PLOTFILE:DEV=PLOT"/
00005022 CMD3(70:11)=815C
00005023 CALL CCNMAND(CMD3,IR1,IR2)
00005030 CMD4(70:11)=815C
00005040 CALL COMMAND(CMD4,IR1,IR2)
00005050 NA=0
00005060 Z=0.
00005100 ISP=0
00005110 NA=NA+1
00005210 DISPLAY " EDITOR <CR> IF NO MORE DATA "
00005220 DISPLAY " AXIS LENGTH ON PLOTS-IN INCHES? "
00005300 READ(5,*)JAXLEN
00005300 DISPLAY " LA-ARRAY CONFIG.,NL=#LAYERS,ISP=#SPACINGS "
00005310 READ(5,*)END=1004)LA,NL,ISP
00005320 Z=Z+1.
00005330 IPS=ISP
00005340 I1=ISP+1
00005350 I2=ISP+2
00005360 IF (LA.EQ.0)GO TO 1967
00005370 IF (ISP.GT.0)ISAVE=ISP
00005380 FORMAT(I1,I4,I5)
00005390 IF ((LA.LE.5).OR.(LA.GT.0))GO TO 1002
00005400 WRITE(4,1003)
00005410 FORMAT(9) INVALID MODE SPECIFIED. LA MUST BE "/
00005420
00005430
00005440
00005450
00005460
00005470
00005480
00005490
00005500
00005510
00005520
00005530
00005540
00005550
00005560
00005570
00005580
00005590
00005600
00005610
00005620
00005630
00005640
00005650
00005660
00005670
00005680
00005690
00005700
00005710
00005720
00005730
00005740
00005750
00005760
00005770
00005780
00005790
00005800
00005810
00005820
00005830
00005840
00005850
00005860
00005870
00005880
00005890
00005900
00005910
00005920
00005930
00005940
00005950
00005960
00005970
00005980
00005990
00006000
00006010
00006020
00006030
00006040
00006050
00006060
00006070
00006080
00006090
00006100
00006110
00006120
00006130
00006140
00006150
00006160
00006170
00006180
00006190
00006200
00006210
00006220
00006230
00006240
00006250
00006260
00006270
00006280
00006290
00006300
00006310
00006320
00006330
00006340
00006350
00006360
00006370
00006380
00006390
00006400
00006410
00006420
00006430
00006440
00006450
00006460
00006470
00006480
00006490
00006500
00006510
00006520
00006530
00006540
00006550
00006560
00006570
00006580
00006590
00006600
00006610
00006620
00006630
00006640
00006650
00006660
00006670
00006680
00006690
00006700
00006710
00006720
00006730
00006740
00006750
00006760
00006770
00006780
00006790
00006800
00006810
00006820
00006830
00006840
00006850
00006860
00006870
00006880
00006890
00006900
00006910
00006920
00006930
00006940
00006950
00006960
00006970
00006980
00006990
00007000
00007010
00007020
00007030
00007040
00007050
00007060
00007070
00007080
00007090
00007100
00007110
00007120
00007130
00007140
00007150
00007160
00007170
00007180
00007190
00007200
00007210
00007220
00007230
00007240
00007250
00007260
00007270
00007280
00007290
00007300
00007310
00007320
00007330
00007340
00007350
00007360
00007370
00007380
00007390
00007400
00007410
00007420
00007430
00007440
00007450
00007460
00007470
00007480
00007490
00007500
00007510
00007520
00007530
00007540
00007550
00007560
00007570
00007580
00007590
00007600
00007610
00007620
00007630
00007640
00007650
00007660
00007670
00007680
00007690
00007700
00007710
00007720
00007730
00007740
00007750
00007760
00007770
00007780
00007790
00007800
00007810
00007820
00007830
00007840
00007850
00007860
00007870
00007880
00007890
00007900
00007910
00007920
00007930
00007940
00007950
00007960
00007970
00007980
00007990
00008000
00008010
00008020
00008030
00008040
00008050
00008060
00008070
00008080
00008090
00008100
00008110
00008120
00008130
00008140
00008150
00008160
00008170
00008180
00008190
00008200
00008210
00008220
00008230
00008240
00008250
00008260
00008270
00008280
00008290
00008300
00008310
00008320
00008330
00008340
00008350
00008360
00008370
00008380
00008390
00008400
00008410
00008420
00008430
00008440
00008450
00008460
00008470
00008480
00008490
00008500
00008510
00008520
00008530
00008540
00008550
00008560
00008570
00008580
00008590
00008600
00008610
00008620
00008630
00008640
00008650
00008660
00008670
00008680
00008690
00008700
00008710
00008720
00008730
00008740
00008750
00008760
00008770
00008780
00008790
00008800
00008810
00008820
00008830
00008840
00008850
00008860
00008870
00008880
00008890
00008900
00008910
00008920
00008930
00008940
00008950
00008960
00008970
00008980
00008990
00009000
00009010
00009020
00009030
00009040
00009050
00009060
00009070
00009080
00009090
00009100
00009110
00009120
00009130
00009140
00009150
00009160
00009170
00009180
00009190
00009200
00009210
00009220
00009230
00009240
00009250
00009260
00009270
00009280
00009290
00009300
00009310
00009320
00009330
00009340
00009350
00009360
00009370
00009380
00009390
00009400
00009410
00009420
00009430
00009440
00009450
00009460
00009470
00009480
00009490
00009500
00009510
00009520
00009530
00009540
00009550
00009560
00009570
00009580
00009590
00009600
00009610
00009620
00009630
00009640
00009650
00009660
00009670
00009680
00009690
00009700
00009710
00009720
00009730
00009740
00009750
00009760
00009770
00009780
00009790
00009800
00009810
00009820
00009830
00009840
00009850
00009860
00009870
00009880
00009890
00009900
00009910
00009920
00009930
00009940
00009950
00009960
00009970
00009980
00009990
00010000
00010010
00010020
00010030
00010040
00010050
00010060
00010070
00010080
00010090
00010100
00010110
00010120
00010130
00010140
00010150
00010160
00010170
00010180
00010190
00010200
00010210
00010220
00010230
00010240
00010250
00010260
00010270
00010280
00010290
00010300
00010310
00010320
00010330
00010340
00010350
00010360
00010370
00010380
00010390
00010400
00010410
00010420
00010430
00010440
00010450
00010460
00010470
00010480
00010490
00010500
00010510
00010520
00010530
00010540
00010550
00010560
00010570
00010580
00010590
00010600
00010610
00010620
00010630
00010640
00010650
00010660
00010670
00010680
00010690
00010700
00010710
00010720
00010730
00010740
00010750
00010760
00010770
00010780
00010790
00010800
00010810
00010820
00010830
00010840
00010850
00010860
00010870
00010880
00010890
00010900
00010910
00010920
00010930
00010940
00010950
00010960
00010970
00010980
00010990
00011000
00011010
00011020
00011030
00011040
00011050
00011060
00011070
00011080
00011090
00011100
00011110
00011120
00011130
00011140
00011150
00011160
00011170
00011180
00011190
00011200
00011210
00011220
00011230
00011240
00011250
00011260
00011270
00011280
00011290
00011300
00011310
00011320
00011330
00011340
00011350
00011360
00011370
00011380
00011390
00011400
00011410
00011420
00011430
00011440
00011450
00011460
00011470
00011480
00011490
00011500
00011510
00011520
00011530
00011540
00011550
00011560
00011570
00011580
00011590
00011600
00011610
00011620
00011630
00011640
00011650
00011660
00011670
00011680
00011690
00011700
00011710
00011720
00011730
00011740
00011750
00011760
00011770
00011780
00011790
00011800
00011810
00011820
00011830
00011840
00011850
00011860
00011870
00011880
00011890
00011900
00011910
00011920
00011930
00011940
00011950
00011960
00011970
00011980
00011990
00020000
00020010
00020020
00020030
00020040
00020050
00020060
00020070
00020080
00020090
00020100
00020110
00020120
00020130
00020140
00020150
00020160
00020170
00020180
00020190
00020200
00020210
00020220
00020230
00020240
00020250
00020260
00020270
00020280
00020290
00020300
00020310
00020320
00020330
00020340
00020350
00020360
00020370
00020380
00020390
00020400
00020410
00020420
00020430
00020440
00020450
00020460
00020470
00020480
00020490
00020500
00020510
00020520
00020530
00020540
00020550
00020560
00020570
00020580
00020590
00020600
00020610
00020620
00020630
00020640
00020650
00020660
00020670
00020680
00020690
00020700
00020710
00020720
00020730
00020740
00020750
00020760
00020770
00020780
00020790
00020800
00020810
00020820
00020830
00020840
00020850
00020860
00020870
00020880
00020890
00020900
00020910
00020920
00020930
00020940
00020950
00020960
00020970
00020980
00020990
00021000
00021010
00021020
00021030
00021040
00021050
00021060
00021070
00021080
00021090
00021100
00021110
00021120
00021130
00021140
00021150
00021160
00021170
00021180
00021190
00021200
00021210
00021220
00021230
00021240
00021250
00021260
00021270
00021280
00021290
00021300
00021310
00021320
00021330
00021340
00021350
00021360
00021370
00021380
00021390
00021400
00021410
00021420
00021430
00021440
00021450
00021460
00021470
00021480
00021490
00021500
00021510
00021520
00021530
00021540
00021550
00021560
00021570
00021580
00021590
00021600
00021610
00021620
00021630
00021640
00021650
00021660
00021670
00021680
00021690
00021700
00021710
00021720
00021730
00021740
00021750
00021760
00021770
00021780
00021790
00021800
00021810
00021820
00021830
00021840
00021850
00021860
00021870
00021880
00021890
00021900
00021910
00021920
00021930
00021940
00021950
00021960
00021970
00021980
00021990
00030000
00030010
00030020
00030030
00030040
00030050
00030060
00030070
00030080
00030090
00030100
00030110
00030120
00030130
00030140
00030150
00030160
00030170
00030180
00030190
00030200
00030210
00030220
00030230
00030240
00030250
00030260
00030270
00030280
00030290
00030300
00030310
00030320
00030330
00030340
00030350
00030360
00030370
00030380
00030390
00030400
00030410
00030420
00030430
00030440
00030450
00030460
00030470
00030480
00030490
00030500
00030510
00030520
00030530
00030540
00030550
00030560
00030570
00030580
00030590
00030600
00030610
00030620
00030630
00030640
00030650
00030660
00030670
00030680
00030690
00030700
00030710
00030720
00030730
00030740
00030750
00030760
00030770
00030780
00030790
00030800
00030810
00030820
00030830
00030840
00030850
00030860
00030870
00030880
00030890
00030900
00030910
00030920
00030930
00030940
00030950
00030960
00030970
00030980
00030990
00040000
00040010
00040020
00040030
00040040
00040050
00040060
00040070
00040080
00040090
00040100
00040110
00040120
00040130
00040140
00040150
00040160
00040170
00040180
00040190
00040200
00040210
00040220
00040230
00040240
00040250
00040260
00040270
00040280
00040290
00040300
00040310
00040320
00040330
00040340
00040350
00040360
00040370
00040380
00040390
00040400
00040410
00040420
00040430
00040440
00040450
00040460
00040470
00040480
00040490
00040500
00040510
00040520
00040530
00040540
00040550
00040560
00040570
00040580
00040590
00040600
00040610
00040620
00040630
00040640
00040650
00040660
00040670
00040680
00040690
00040700
00040710
00040720
00040730
00040740
00040750
00040760
00040770
00040780
00040790
00040800
00040810
00040820
00040830
00040840
00040850
00040860
00040870
00040880
00040890
00040900
00040910
00040920
00040930
00040940
00040950
00040960
00040970
00040980
00040990
00050000
00050010
00050020
00050030
00050040
00050050
00050060
00050070
00050080
00050090
00050100
00050110
00050120
00050130
00050140
00050150
00050160
00050170
00050180
00050190
00050200
00050210
00050220
00050230
00050240
00050250
00050260
00050270
00050280
00050290
00050300
00050310
00050320
00050330
00050340
00050350
00050360
00050370
00050380
00050390
00050400
00050410
00050420
00050430
00050440
00050450
00050460
00050470
00050480
00050490
00050500
00050510
00050520
00050530
00050540
00050550
00050560
00050570
00050580
00050590
00050600
00050610
00050620
00050630
00050640
00050650
00050660
00050670
00050680
00050690
00050700
00050710
00050720
00050730
00050740
00050750
00050760
00050770
00050780
00050790
00050800
00050810
00050820
00050830
00050840
00050850
00050860
00050870
00050880
00050890
00050900
00050910
00050920
00050930
00050940
00050950
00050960
00050970
00050980
00050990
00060000
00060010
00060020
00060030
00060040
00060050
00060060
00060070
00060080
00060090
00060100
00060110
00060120
00060130
00060140
00060150
00060160
00060170
00060180
00060190
00060200
00060210
00060220
00060230
00060240
00060250
00060260
00060270
00060280
00060290
00060300
00060310
00060320
00060330
00060340
00060350
00060360
00060370
00060380
00060390
00060400
00060410
00060420
00060430
00060440
00060450
00060460
00060470
00060480
00060490
00060500
00060510
00060520
00060530
00060540
00060550
0
```

0002

```

00012000      &"HE TW,IK5 ")
00013000      GO TO 1000
00014000      CONTINUE
00015000      DO 10 I=1,100
00016000      FSCH(I)=0.
00017000      SCH(I)=0.
00018000      FFNER(I)=0.
00019000      WENNER(I)=0.
00020000      NT(I)=0.
00021000      NR(I)=0.
00022000      CK(I)=0.
00023000      NID(I)=0.
00024000      DO 20 I=1,2
00025000      DO 30 J=1,2001
00026000      P(I,J)=0.
00027000      H(I,J)=0.
00028000      Q(J)=0.
00029000      OK(J)=0.
00030000      NLM=NL-1
00031000      DISPLAY " LAYER THICKNESSES "
00032000      ACCEPT(NT(I),I=1,20)
00033000      IF (NLM.LE.20)GO TO 6123
00034000      ACCEPT(NT(I),I=21,40)
00035000      IF (NLM.LE.40)GO TO 6123
00036000      ACCEPT(NT(I),I=41,60)
00037000      IF (NLM.LE.60)GO TO 6123
00038000      ACCEPT(NT(I),I=61,80)
00039000      DISPLAY " LAYER RESISTIVITIES "
00040000      ACCEPT(NR(I),I=1,20)
00041000      IF (NLM.LE.20)GO TO 9876
00042000      ACCEPT(NR(I),I=21,40)
00043000      IF (NLM.LE.40)GO TO 9876
00044000      ACCEPT(NR(I),I=41,60)
00045000      IF (NLM.LE.60)GO TO 9876
00046000      ACCEPT(NR(I),I=61,80)
00047000      IF ISP .LE. 0 USE OLD SPACINGS
00048000      IF (ISP)2000,9000,2002
00049000      DISPLAY " # OF ELECTRODE SPACINGS "
00050000      ACCEPT(SP(I),I=1,15)
00051000      IF (ISP.LE.15) GO TO 4785
00052000      ACCEPT(SP(I),I=16,30)
00053000      IF (ISP.LE.30) GO TO 4785
00054000      ACCEPT(SP(I),I=31,45)
00055000      IF (ISP.LE.45)GO TO 4785
00056000      ACCEPT(SP(I),I=46,60)
00057000      IF (ISP.LE.60)GO TO 4785
00058000      ACCEPT(SP(I),I=61,75)
00059000      DO 2222 II=1,ISP
00060000      SAVSP(II)=SP(II)
00061000      CONTINUE
00062000      GO TO 2200
00063000      ISP=ISAVE
00064000      DO 1111 II=1,ISAVE
00065000      SP(II)=SAVSP(II)
00066000      CONTINUE
00067000      1111
00068000      2200
    
```

PA 0003

```

00044000 102 FORMAT(H110)
00045000 100 FORMAT(AF10.6)
00046000 WRITE(4,1)
00047000 1 FORMAT("1", "THESE ARE LA (FH THICKNESSES ")
00048000 212 FORMAT(" ",10110)
00049000 WRITE(4,212)(NT(I),I=1,NLM)
00050000 WRITE(4,2)
00051000 2 FORMAT("0", "THESE ARE LAYER RESISTIVITIES")
00052000 WRITE(4,212)(NR(I),I=1,NL)
00053000 WRITE(4,3)
00054000 3 FORMAT("0", "THESE ARE THE ELECTRODE SPACINGS")
00055000 WRITE(4,222)(SP(I),I=1,ISP)
00056000 C COMPUTE THE RESISTIVITY CONTRASTS
00057000 DO 40 I=1,NLM
00058000 CK(I)=FLOAT(NR(I+1)-NR(I))/FLOAT(NR(I+1)+NR(I))
00059000 WRITE(4,111)
00060000 111 FORMAT("0", "THESE ARE RESISTIVITY CONTRASTS")
00061000 WRITE(4,222)(CK(I),I=1,NLM)
00062000 222 FORMAT(" ",10F10.6)
00063000 C NOW COMPUTE THE COEFFICIENTS P&H
00064000 C FEED IN KNOWN COEFFICIENTS P(1)&H(1)
00065000 P(1,1)=0.
00066000 H(1,1)=1.0
00067000 IX=2
00068000 IY=1
00069000 C BUT FIRST WE MUST COMPUTE THE DEPTHS TO VARIOUS LAYERS
00070000 NTD(1)=NT(1)
00071000 DO 50 I=2,NLM
00072000 IF(NLM.EQ.1)GO TO 2143
00073000 NTD(I)=NTD(I-1)+NT(I)
00074000 WRITE(4,333)
00075000 50 FORMAT("0", "THESE ARE THE DEPTHS TO THE TOPS OF "/IX
00076000 2143 6" THE MODEL LAYERS ")
00077000 WRITE(4,212)(NTD(I),I=1,NLM)
00078000 C WE HAVE JUST COMPUTED THE DEPTHS TO THE TOP I+1
00079000 C LAYER NOW WE ACTUALLY COMPUTE THE COEFFICIENTS P&H
00080000 DO 60 I=1,NLM
00081000 L=NTD(I)+1
00082000 DO 65 N=1,L
00083000 P(IX,N)=P(IY,N)+CK(I)*H(IY,L-N+1))
00084000 H(IX,N)=H(IY,N)+CK(I)*P(IY,L-N+1))
00085000 IX=IX+((-1)**I)
00086000 IY=IY-((-1)**I)
00087000 KOUNT=I+1
00088000 IX=IX+((-1)**KOUNT)
00089000 IY=IY-((-1)**KOUNT)
00090000 444 FOP&H("0", "THESE ARE THE COEFFICIENTS P")
00091000 555 FORMAT("0", "THESE ARE THE COEFFICIENTS H")
00092000 C IN THE ABOVE COMPUTATION OF P&H, N TAKES ON VALUES
00093000 C FROM 1 TO THE SUM OF ALL LAYER THICKNESSES
00094000 C ALLP(N)&HN) FOR N .GT. THE SUM OF THE THICKNESSES
00095000 C NOW COMPUTE THE COEFFICIENTS Q(N)
00096000 QK(1)=0.
00097000 Q(1)=P(IX,2)
00098000 NLK=NTD(MLM)
00099000 DO 70 I=2,NLK
00100000 KX=I-1

```

PAL 0004

```

00090000 DO 80 J=1,KX
00091000 M=J+1
00092000 STOR=(P(IX,M)-H(IX,M))*Q(I-J)
80 00092100 OK(I)=OK(I)+STOR
00092200 N=I+1
70 00092300 Q(I)=P(IX,N)+OK(I)
00092310 C THE ABOVE COMPUTES Q(N) FOR N=1 L.T. TOTAL LAYER THICK
00092320 C NESSES
00092400 NLJ=NTD(NLM)+1
00092410 NDC=2000
00092420 IF (NT(1).LE.30)NDC=300
00092500 DO 90 I=NLJ,ISP
00092600 KY=I-1
00092700 DO 95 J=1,NLK
00092800 M=J+1
95 00092900 STOR=(P(IX,M)-H(IX,M))*G(I-J)
00093000 OK(I)=OK(I)+STOR
00094000 N=I+1
90 00095000 Q(I)=P(IX,N)+OK(I)
666 00096000 FORMAT('000',)HERE ARE THE FIRST 500 COEFFICIENTS Q(N)
00097000 IF (LA.EQ.1)GO TO 11
C NOW WE HAVE COMPUTED THE COEFFICIENTS Q(N) NECESSARY
00097100 C FOR OBTAINING THE VALUES FOR OUR RESISTIVITY OR POTEN
00097200 C TIAL FUNCTION CURVES
00097300 C NOW WE WILL GO TO THE ALGORITHM WHICH WILL GIVE US OUR
00097400 C DESIRED VALUES FOR THE PARTICULAR ELECTRODE CONFIGURA
00097500 C TION WE HAVE CHOSEN
00097600 C
00098000 12 ABC=LA
00099000 DO 150 I=1,ISP
00100000 WENNER(I)=0.
00101000 DO 155 J=1,1500
00102000 AA=(FLOAT(J)*FLOAT(J))/(ISP(I)*SP(I))
00103000 BB=4.*AA
00104000 CC=(1.+BB)**(-.5)*10.
00105000 DD=(1.+AA)**(-.5)*10.
155 00106000 WENNER(I)=Q(J)*((2.*CC)-DD)+WENNER(I)
150 00107000 FENNER(I)=1.+2.*WENNER(I)
00108000 J=1500
00109000 DO 160 I=1,ISP
00110000 ERR(I)=(3*SP(I)**3)/(FLOAT(BB)*J)*FLOAT(J)
00111000 AER(I)=ERR(I)/FENNER(I)
160 00112000 CONTINUE
00113000 WRITE(4,885)
00114000 WRITE(4,886) (ERR(I), I=1,ISP)
00115000 WRITE(4,777)
00116000 WRITE(4,1000) (AER(I), I=1,ISP)
00117000 DO 165 I=1,ISP
00118000 BER=AER(I)
00119000 IF (BER.GT.(.05))160 TO 170
00120000 CONTINUE
165 00121000 GO TO 994
00122000 BER=0.
170 00123000 DO 175 I=1,ISP
00124000 DO 180 J=1501,2000
00125000 AA=(FLOAT(J)*FLOAT(J))/(SP(I)*SP(I))
00126000 BB=4.*AA
00127000 CC=(1.+BB)**(-.5)

```

PZ 0605

```

00128000 DD=(1.+AA)**(-.5)
00129000 WFNMR(I)=0(J)*(P.*CC)-(DI)+WEIRER(I)
00130000 FENNER(I)=1.+2.*WFNMR(I)
00131000 J=2000
00132000 DO 185 I=1,ISP
00133000 ERR(I)=(3*SP(I)**3)/(FLOAT(P*J)*FLOAT(J))
00134000 AER(I)=ERR(I)/FENNER(I)
00135000 CONTINUE
00136000 WRITE(4,RR4)
00137000 WRITE(4,RR5)(ERR(I),I=1,ISP)
00138000 WRITE(4,RR8)
00139000 WRITE(4,103)(AER(I),I=1,ISP)
00140000 WRITE(4,900)
00141000 FORMAT('00',"HERE ARE THE APPARENT RESISTIVITIES DIVIDED"/IX
00142000 * BY THE RESISTIVITY OF THE FIRST LAYER FOR THE WFNMR"/IX
00143000 * CONFIGURATION**)
00144000 WRITE(4,108)(FENNER(I),I=1,ISP)
00145000 GO TO 998
00146000 WRITE(4,RR9)
00147000 WRITE(4,108)(FENNER(I),I=1,ISP)
00148000 GO TO 998
00149000 I=A1
00150000 DO 105 I=1,ISP
00151000 SCH(I)=0.
00152000 DO 110 J=1,1500
00153000 SCH(I)=0(J)*(1+(4*(FLOAT(J)*FLOAT(J))/SP(I)**2))**(-1.5)+SCH(I)
00154000 FSCH(I)=1+2*SCH(I)
00155000 J=1500
00156000 DO 120 I=1,ISP
00157000 ERR(I)=(SP(I)**3)/(FLOAT(P*J)*FLOAT(J))
00158000 AER(I)=ERR(I)/FSCH(I)
00159000 CONTINUE
00160000 WRITE(4,RR5)
00161000 FORMAT('00',"THESE ARE THE ERRORS FOR 1500 0(N)")
00162000 WRITE(4,RR6)(ERR(I),I=1,ISP)
00163000 FORMAT('00',"10E12.4)
00164000 WRITE(4,777)
00165000 FORMAT('00',"HERE ARE THE VALUES OF THE ERROR DIVIDED"/IX
00166000 * BY THE COMPUTED VALUE FOR 1500 TERMS))
00167000 WRITE(4,108)(AER(I),I=1,ISP)
00168000 DO 121 I=1,ISP
00169000 WERAFR(I)
00170000 IF (ERR.GT..05)GO TO 176
00171000 CONTINUE
00172000 GO TO 887
00173000 WER=0.
00174000 DO 125 I=1,ISP
00175000 DO 130 J=1501,2000
00176000 SCH(I)=0(J)*(1+(4*(FLOAT(J)*FLOAT(J))/SP(I)**2))**(-1.5)+SCH(I)
00177000 FSCH(I)=1+2*SCH(I)
00178000 J=2000
00179000 DO 135 I=1,ISP
00180000 ERR(I)=(SP(I)**3)/(FLOAT(P*J)*FLOAT(J))
00181000 AER(I)=ERR(I)/FSCH(I)
00182000 WRITE(4,RR6)
00183000 FORMAT('00',"THESE ARE THE ERRORS FOR 3000 0(N)")
00184000 WRITE(4,RR6)(ERR(I),I=1,ISP)

```

P2 0006

```

00195000 WRITE(4,ERR)
00196000 R88 FORMAT('0',)HERE ARE THE VALUES OF THE ERROR DIVIDED"/
00197000 WHY THE COMPUTED VALUE FOR 3000 TERMS"
00198000 WRITE(4,108)(AER(I),I=1,ISP)
00199000 FORMAT(" ",10F12.4)
00199000 R87 WRITE(4,ERR)
00199000 R89 FORMAT('0',)HERE ARE THE VALUES FOR THE APPARENT RESISTI"/
00199000 R90 WHY THE COMPUTED VALUE FOR 3000 TERMS"
00199000 R91 WRITE(4,108)(AER(I),I=1,ISP)
00199000 R92 WRITE(4,108)(FSC(I),I=1,ISP)
00199000 R93 DO 1090 I=1,ISP
00199000 R94 FENNER(I)=FENNER(I)*(NR(I))
00199000 R95 DO 1091 I=1,ISP
00199000 R96 FEN(I)=FENNER(I)
00199000 R97 DO 1239 I=1,ISP
00199000 R98 FENNER(I)=(ARS(FENNER(I)))
00199000 R99 SP(I)=ARS(SP(I))
00199000 R100 IF(NA.EQ.1)GO TO 778
00199000 R101 GO TO 772
00199000 R102 CALL PLOTS(INUFF,500)
00199000 R103 CALL PLOT(0.,0.,-3)
00199000 R104 CALL SCALOG(SP,AXLEN,ISP,1)
00199000 R105 SPIN=SP(11)
00199000 R106 SPOFLT=SP(12)
00199000 R107 CALL SCALOG(FENNER,AXLE%,ISP,1)
00199000 R108 FMIN=FENNER(11)
00199000 R109 FDELT=FENNER(12)
00199000 R110 FEN(11)=FENNER(11)
00199000 R111 FEN(12)=FENNER(12)
00199000 R112 CALL LGAXIS(0.,0.,IMLSS,-10,AXLEN,0.,SP(11),SP(12))
00199000 R113 CALL LGAXIS(0.,0.,IRES,20,AXLEN,0.,FENNER(11),FENNER(12))
00199000 R114 CALL LGLINE(SP(1),FEN(1),ISP,1,1,3,0)
00199000 R115 CALL LGLINE(SP(1),FEN(1),ISP,1,1,3,0)
00199000 R116 GO TO 1000
00199000 R117 SP(11)=SPMIN
00199000 R118 SP(12)=SPOFLT
00199000 R119 FENNER(11)=FMIN
00199000 R120 FENNER(12)=FDELT
00199000 R121 CALL LGLINE(SP(1),FEN(1),ISP,1,1,3,0)
00199000 R122 CALL PLOT(0.,0.,-3)
00199000 R123 GO TO 1000
00199000 R124 DISPLAY " NUMBER OF FIELD E-SPACINGS "
00199000 R125 HEAD(5,*)IFEP
00199000 R126 DISPLAY "WHAT ARE FIELD E-SPACINGS? "
00199000 R127 ACCEPT(FSP(1),I=1,IFEP)
00199000 R128 DISPLAY " WHAT ARE FIELD RESISTIVITIES ? "
00199000 R129 ACCEPT(FRES(1),I=1,10)
00199000 R130 IF (IFEP.LE.10)GO TO 1978
00199000 R131 ACCEPT(FRES(I),I=1,IFEP)
00199000 R132 I1=IFEP+1
00199000 R133 I2=IFEP+2
00199000 R134 FSP(11)=SPMIN
00199000 R135 FSP(12)=SPOFLT
00199000 R136 FRES(11)=FMIN
00199000 R137 FRES(12)=FDELT
00199000 R138 DO 17 I=1,IFEP+2
00199000 R139 FSP(I)=ALOG(FSP(I))
00199000 R140 FRES(I)=ALOG(FRES(I))
00199000 R141 17

```

PAGE 0007

00194920 CALL LGLINE(FSP(1),FRS(1),FFP.1*1.3.0)
00194930 CALL PLOT(0.,0.,-3)
00194940 GO TO 1000
00195000 1004 STOP
00196000 END

*** NO ERRORS. NO WARNINGS. PROGRAM UNIT COMPILED ***
COMPILATION TIME 11.941 SECONDS ELAPSED TIME 24.542 SECONDS
TOTAL COMPILATION TIME 0:00:13
TOTAL ELAPSED TIME 0:00:30

APPENDIX B

Results from the Computer Program in Appendix A

THESE ARE LAYER THICKNESSES
 12 50 400

THESE ARE LAYER RESISTIVITIES
 1000 200 600 300

THESE ARE THE ELECTRODE SPACINGS
 2.000000 4.000000 6.000000 8.000000 10.000000 15.000000 20.000000 25.000000 30.000000 35.000000
 40.000000 45.000000 50.000000 60.000000 70.000000 80.000000 90.000000 100.000000 120.000000 150.000000
 170.000000 200.000000 240.000000 270.000000 300.000000 350.000000 400.000000 450.000000 500.000000 600.000000
 700.000000 800.000000 900.000000 #####

THESE ARE RESISTIVITY CONTRASTS
 -.666667 .636364 -.500000

THESE ARE THE DEPTHS TO THE TOPS OF
 THE MODEL LAYERS
 12 62 462

THESE ARE THE ERRORS FOR 1500 G(M)

.1333E-05	.1067E-04	.7400E-04	.8533E-04	.5625E-03	.1333E-02	.2604E-02	.4500E-02	.7146E-02
.1067E-01	.1519E-01	.2604E-01	.3600E-01	.5717E-01	.1215E+00	.1667E+00	.2880E+00	.5625E+00
.8188E+00	.1333E+01	.2304E+01	.3280E+01	.4500E+01	.1067E+02	.1519E+02	.2083E+02	.3600E+02
.5717E+02	.8533E+02	.1215E+03	.1667E+03	.2880E+03	.5625E+03			

THESE ARE THE VALUES OF THE ERROR DIVIDED
 BY THE COMPUTED VALUE FOR 1500 TERMS

.0000	.0000	.0001	.0014	-.0003	-.0004	-.0006	-.0008	-.0012
-.0014	-.0025	-.0036	-.0055	-.0148	-.0219	-.0312	-.0583	-.1272
-.1986	-.3564	-.6015	-1.0623	-2.7101	-4.3295	-6.4622	-9.1318	-16.1071
-25.2765	-36.7091	-50.5533	-67.0632	-109.0838	-199.0497			

THESE ARE THE APPARENT RESISTIVITIES DIVIDED
 BY THE RESISTIVITY OF THE FIRST LAYER FOR THE WENNER
 CONFIGURATION

.9291	.8455	.5779	.0600	-2.2167	-3.6704	-4.7152	-5.3944	-5.8050
-5.0345	-6.1422	-8.1714	-6.1026	-5.7490	-5.5427	-5.3361	-4.9423	-4.4222
-4.1400	-3.2409	-3.0822	-3.0822	-2.6367	-2.4637	-2.3502	-2.2814	-2.2350
-2.2617	-2.1324	-2.0400	-2.0400	-2.0400				

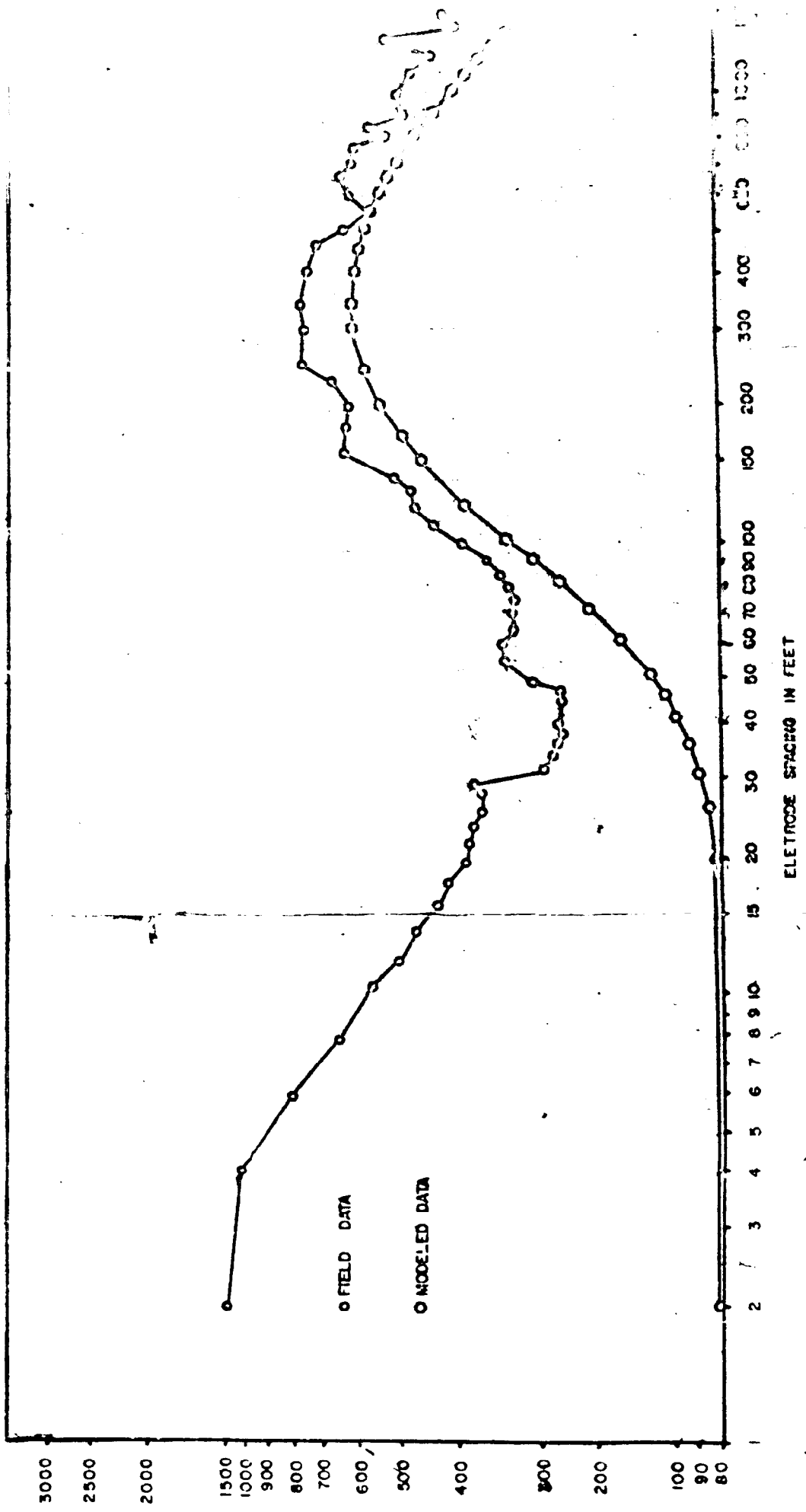


FIGURE 17 PLOT OF APPARENT RESISTIVITY VS ELECTRODE SPACING FOR MODELED AND FIELD DATA